Photoinduced (ultra fast) electronic and nuclear dynamics in molecules

Françoise Remacle
Theoretical physical Chemistry
University of Liège

Photoinduced : Excitation by a short strong atto to few fs pulses

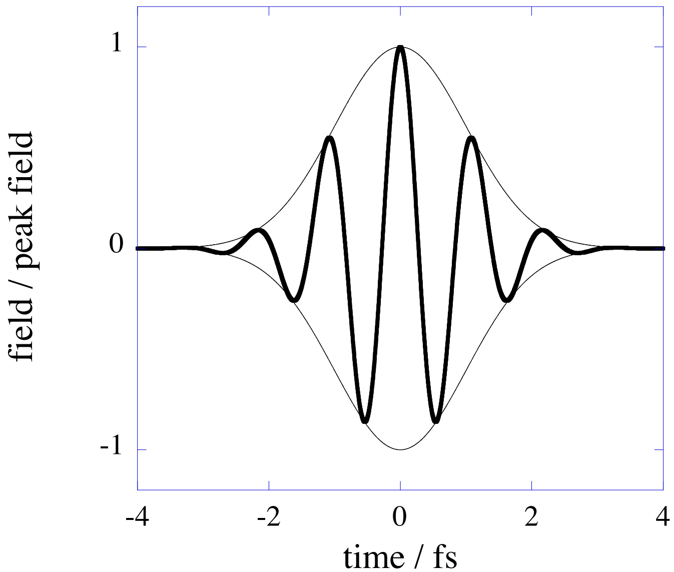

sub to a few femtoseconds, strong, few cycle, ultrashort, optical pulses

$$\mathbf{E}(t) = \mathbf{E}\ f(t)\cos(\omega t + \phi)$$

- $f(t)$ is the envelope
- ω is the carrier frequency
- $\mathbf{E}$ is the electric field
- ϕ is the CEP phase

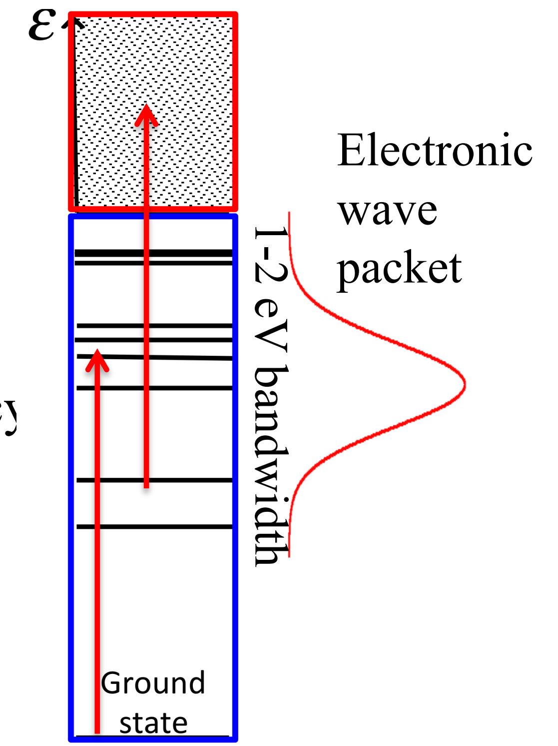

Coherent electronic wave packet is built by the excitation

Polyatomic molecules : Dense manifold of electronic (vibronic) states

Multiphoton processes are possible

- **Photoexcitation** of the neutral electronic states
- **Photoionization** to the states of the cation

Attopulse : Investigate a purely electronic time scale before the nuclei have time to significantly respond

Ultrafast electronic excitation followed by ultrafast electronic reorganization before the nuclei have time to significantly move

Attopulses can induce ultrafast (sudden) ionization

For modular systems : Ultrafast charge migration in cationic states before significant rearrangement of the nuclei

Pioneered by Weinkauf and Schlag before the engineering of attopulses

Site selective dissociation of peptide ions following localized ionization
(Schlag and Weinkauf : J. Phys. Chem. **100**, 18567 (1996))

Charge migration following sudden ionization in modular systems

Remacle, F.; Levine, R. D.; Ratner, M. A., Charge Directed Reactivity: A Simple Electronic Model Exhibiting Site Selectivity for the Dissociation of Ions. *Chem. Phys. Lett.* **1998,** *285*, 25-33.
Remacle, F.; Levine, R. D., Charge Migration and Control of Site Selective Reactivity: The Role of Covalent and Ionic States. *J. Chem. Phys.* **1999,** *110*, 5089-5099.
Remacle, F.; Levine, R. D.; Schlag, E. W.; Weinkauf, R., Electronic Control of Site Selective Reactivity: A Model Combining Charge Migration and Dissociation. *J. Phys. Chem. A* **1999,** *103*, 10149-10158.

Cederbaum, L. S.; Zobeley, J., Ultrafast Charge Migration by Electron Correlation. *Chem. Phys. Lett.* **1999,** *307*, 205-210.
Lünnemann, S.; Kuleff, A. I.; Cederbaum, L. S., Ultrafast Charge Migration in 2-Phenylethyl-N,N-Dimethylamine. *Chemical Physics Letters* **2008,** *450*, 232-235.
Hennig, H.; Breidbach, J.; Cederbaum, L. S., Electron Correlation as the Driving Force for Charge Transfer: Charge Migration Following Ionization in N-Methyl Acetamide. *J. Phys. Chem. A* **2005,** *109*, 409-414.

Charge migration following sudden ionization in modular systems

A non stationary electronic state of the cation is built at the step of sudden ionization, that coherently beats in time on a few fs time scale

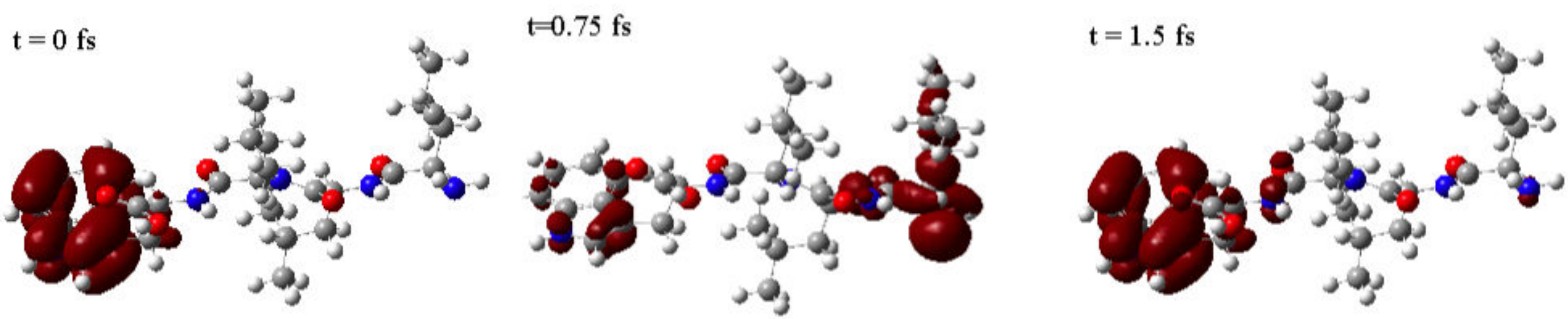

sudden ionization of the HOMO of Trp

ultrafast hole migration, faster than a vibrational period

An electronic time scale for chemistry

F. Remacle and R. D. Levine,
Proc. Natl. Acad. Sci. USA **103**, 6793 (2006)

Pump-probe attosecond experiments give access to this very fast electronic time scale

Experimental probing of charge migration in polyatomic molecules

Atto second pump and probe is not yet easily available

Indirect probing using a combination of XUV atto pulses and NIR fs ones, detecting oscillations in fragment yield with mass spectrometry

Calegari et al Science 2014 : cation of phenylalanine attosecond pump (XUV 300 as)- second ionization 4fs VIS-NIR oscillations in the doubly charge fragments.

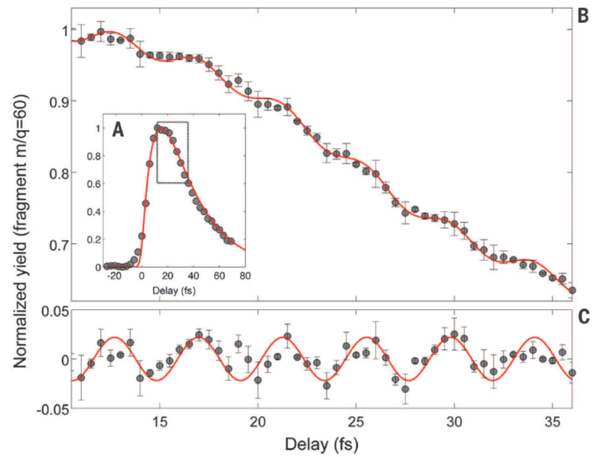

Niedel et al, PRL 2013 (NIR pump and ATP XUV probe), oscillations in the fragment yield that follow the fs oscillations of the NIR electric field.

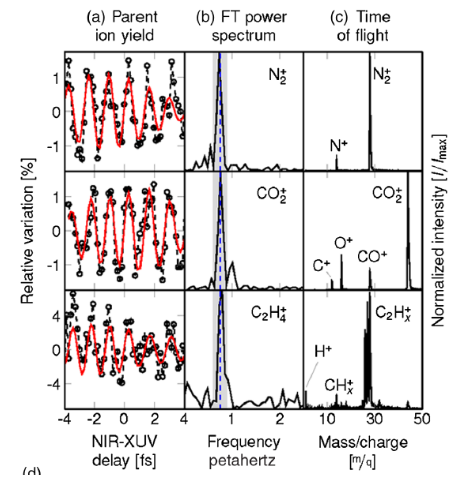

See also recent review, Martin et al Chem Rev 2017.

Direct probing of few fs purely electronic non equilibrium dynamics using a single pulse for pumping and probing

- angularly resolved photoelectron spectra of C_{60} by a few fs strong IR pulse monitored as a function of the CEP of the pulse that acts as a clock.
- HHG spectra of iodoacetylene as a function of the polarization and of the wavelength of the IR pulse.

Joint theory-experimental studies

Partitioning technique

$$\begin{cases} \mathbf{1} = \mathbf{Q} + \mathbf{P} \\ \mathbf{QP} = 0, \mathbf{Q}^2 = \mathbf{Q} \ \text{ and } \mathbf{P}^2 = \mathbf{P} \end{cases}$$

Q : Bound subspace

$$\mathbf{Q} = \sum_I \left| \Psi_I^{Neut} \right\rangle \left\langle \Psi_I^{Neut} \right|$$

P : Ionized subspace

$$\mathbf{P} = \sum_K \sum_{\mathbf{k}_1} \left| \Psi_K^{Cat}, \chi^{\perp}_{\mathbf{k}_1} \right\rangle \left\langle \Psi_K^{Cat}, \chi^{\perp}_{\mathbf{k}_1} \right|$$

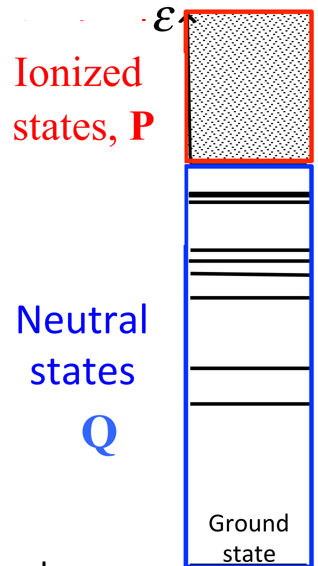

Field free electronic states

Neutral Ψ_I^{Neut} and cation Ψ_K^{Cat}

1. small to medium molecules
Complete active space average (CAS-SCF)

2. medium to large molecules
Linear response TD-DFT (possibility to compute a large number of states)

- $\chi^{\perp}_{\mathbf{k}_1}$: plane waves orthogonalized to the MO's of the neutral
- antisymmetrized wave functions
- Discretization of the continuum in energy and solid angle.

R. D. Levine, *Quantum mechanics of molecular rate processes* (Clarendon Press, 1969); H. Feshbach, Annals of Physics **19**, 287 (1962).

Excitation and ionization dynamics

Partitioned time dependent Schrödinger equation

$$i\begin{pmatrix} d\mathbf{Q}\Psi(t)/dt \\ d\mathbf{P}\Psi(t)/dt \end{pmatrix} = \begin{pmatrix} \mathbf{Q}H(t)\mathbf{Q} & \mathbf{Q}H(t)\mathbf{P} \\ \mathbf{P}H(t)\mathbf{Q} & \mathbf{P}H(t)\mathbf{P} \end{pmatrix}\begin{pmatrix} \mathbf{Q}\Psi(t) \\ \mathbf{P}\Psi(t) \end{pmatrix}$$

Time-dependent wavefunction

$$\left|\Psi(t)\right\rangle = c_I^{Neut}(t)\left|\Psi_I^{Neut}\right\rangle + c_{K,\mathbf{k}_1}^{Cat}(t)\left|\Psi_K^{Cat},\chi_{\mathbf{k}_1}^{\perp}\right\rangle$$

B. Mignolet, R. D. Levine, and F. Remacle, Physical Review A (R) **89**, 021403 (2014)
B. Mignolet, T. Kùs, and F. Remacle, in *Imaging and Manipulating Molecular Orbitals*, edited by L. Grill and C. Joachim (Springer Berlin Heidelberg, 2013), p. 41.

Photoexcitation and photoionization dynamics

Pump and probe pulses $$\mathbf{E}(t) = -\sum_{i=1}^{2} \mathbf{E}_i f_{0,i}\, e^{-(t-t_i)^2/\sigma_i^2} \left[\cos(\omega_i t) - \frac{2(t-t_i)\sin(\omega_i t)}{\omega_i \sigma_i^2} \right]$$

- Dynamics in the bound states $\mathbf{Q}H(t)\mathbf{Q}$

$$H(t) = H^0_{ele}(\mathbf{r}) - \boldsymbol{\mu}\cdot\mathbf{E}(t)$$

$$\left\langle \Psi_I^{Neut} \middle| H(t) \middle| \Psi_J^{Neut} \right\rangle = \delta_{I,J} E_I^{Neut} - \mathbf{E}(t)\boldsymbol{\mu}_{I-J}$$

- Dynamics in the ionized states : $\mathbf{P}H(t)\mathbf{P}$

$$H(t) \approx \left(H_{ele}^{Cat} - \boldsymbol{\mu}^{Cat}\cdot\mathbf{E}(t) \right) - \left(\frac{1}{2}\mathbf{p}_1^2 - \mathbf{E}(t)\mathbf{r} \right)$$

$$\mathbf{P}H(t)\mathbf{P} = \mathbf{P}\left(H_{ele}^{0Cat} - \boldsymbol{\mu}^{Cat}\cdot\mathbf{E}(t) \right)\mathbf{P} - \mathbf{P}\left(\frac{1}{2}\mathbf{p}_1^2 - \mathbf{E}(t)\mathbf{r} \right)\mathbf{P}$$

Basis of plane waves for the ionized electron

- Ionization dynamics : $\mathbf{P}H(t)\mathbf{Q}$ and $\mathbf{Q}H(t)\mathbf{P}$

$$\left\langle \Psi_I^{Neut} \middle| H(t) \middle| \Psi_K^{Cat}, \chi^{\perp}{}_{\mathbf{k}_1} \right\rangle = \mathbf{E}(t) \left\langle \phi_{I-K}^{Dyson} \middle| \mathbf{r} \middle| \chi^{\perp}{}_{\mathbf{k}_1} \right\rangle$$

$$\phi_{IK}^{Dyson} = \sqrt{n} \int d\mathbf{r}_2 \ldots d\mathbf{r}_n \Psi_I^{Neut*}(\mathbf{r}_1,\ldots\mathbf{r}_n)\Psi_K^{Cat}(\mathbf{r}_2,\ldots\mathbf{r}_n)$$

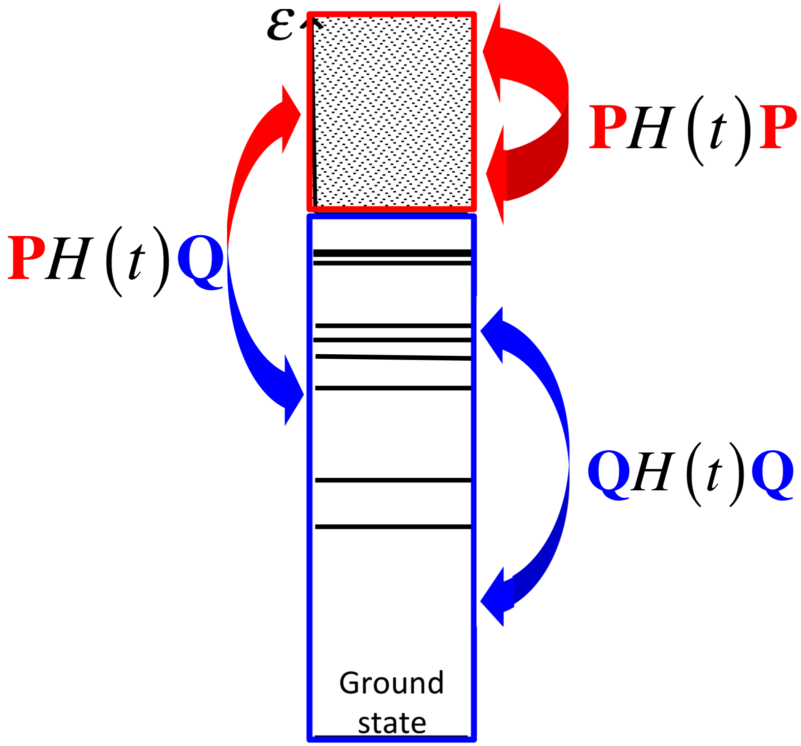

B. Mignolet, R. D. Levine, and F. Remacle, Physical Review A (R) **89**, 021403 (2014)
B. Mignolet, T. Kùs, and F. Remacle, in *Imaging and Manipulating Molecular Orbitals*, edited by L. Grill and C. Joachim (Springer Berlin Heidelberg, 2013), p. 41.

Coherent motion of the electronic density in LiH induced by a polarized UV short pump pulse

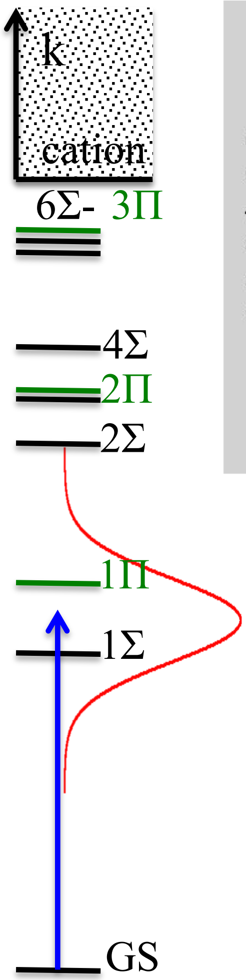

polarization along z

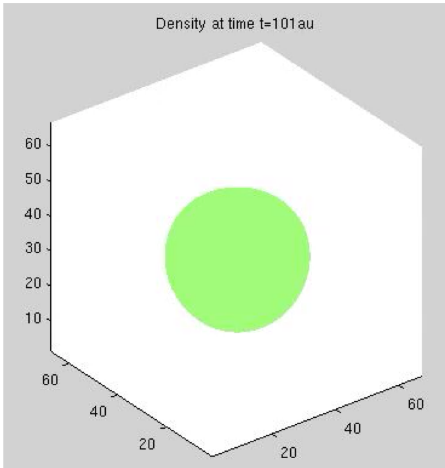

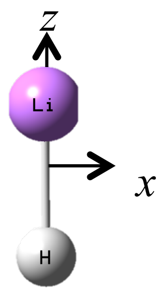

polarization in (x,z)

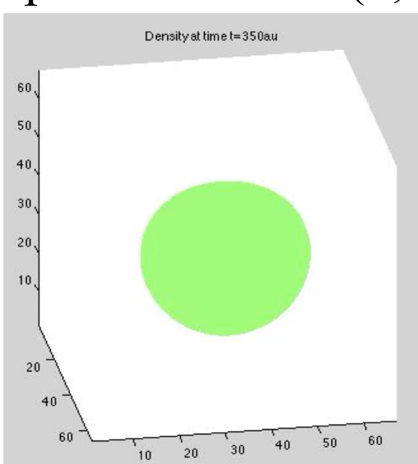

$$\mu_z(t) = \langle \Psi(t) | z | \Psi(t) \rangle$$

polarization along z

polarization in (x,z)

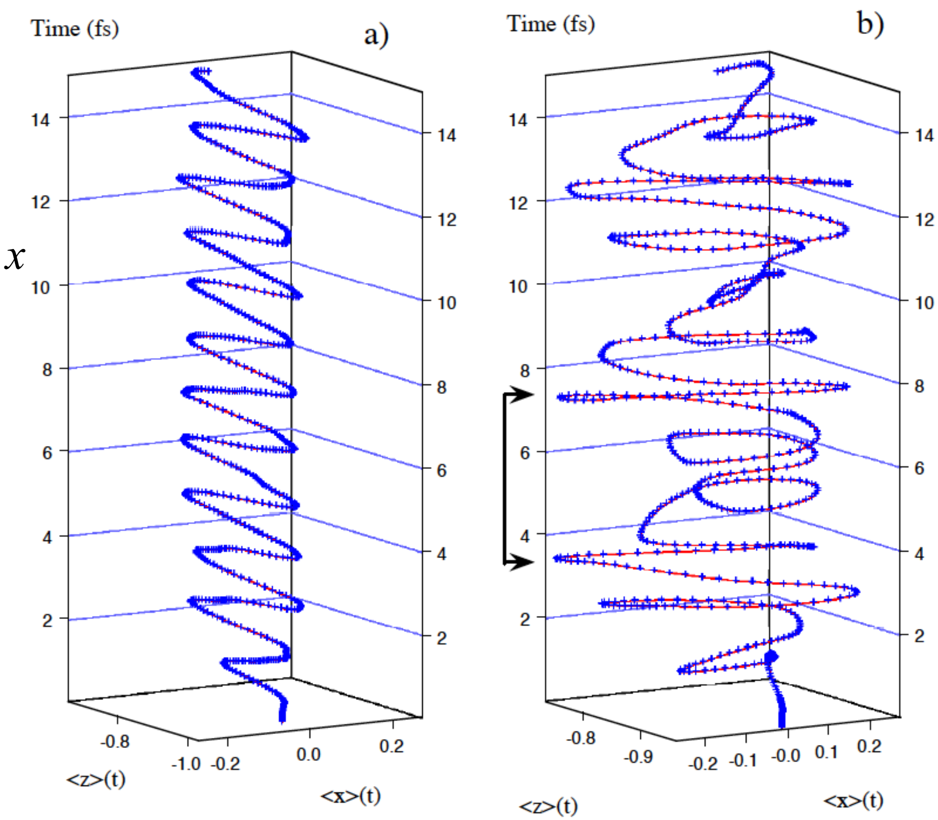

ω= 0.133 au, |E| = 0.025 au (2 10^{13} W/cm^2), σ=0.68 fs

F. Remacle, M. Nest, R.D. Levine, Phys. Rev. Lett., 99 (2007) TD-CAS (4,5)

Probing the electronic dynamics in the iodoacetylene cation using HHG

Kraus, P. M., B. Mignolet, D. Baykusheva, A. Rupenyan, L. Horný, E. F. Penka, G. Grassi, O. I. Tolstikhin, J. Schneider, F. Jensen, L. B. Madsen, A. D. Bandrauk, F. Remacle and H. J. Wörner (2015). "Measurement and laser control of attosecond charge migration in ionized iodoacetylene." Science **350**(6262): 790-795.

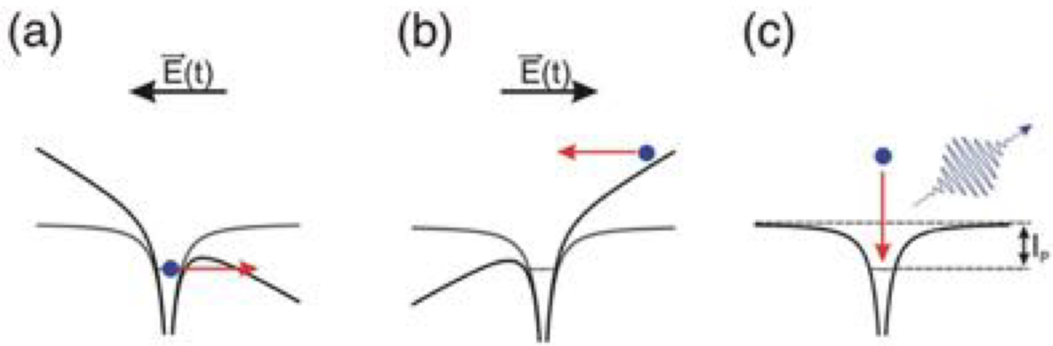

Three step model

P. Corkum

HHG

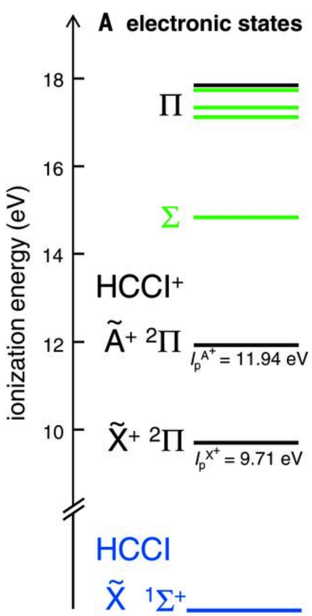

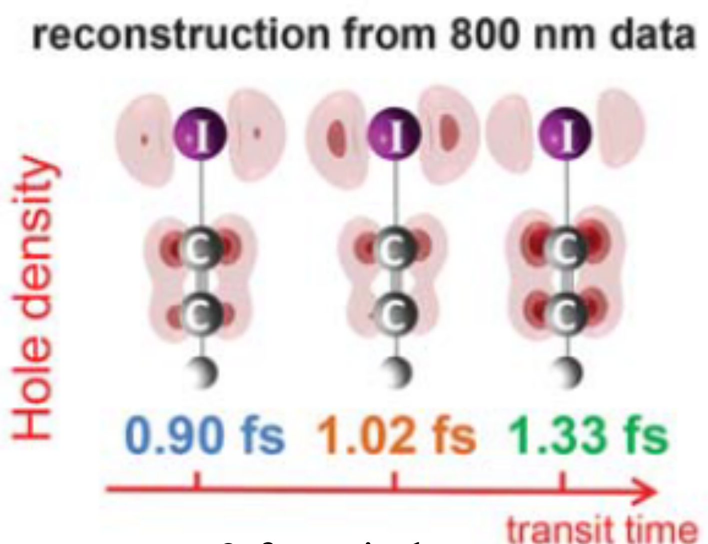

2 fs period

- ratio of intensities of the emitted harmonic aligned and anti-aligned
- phase of the harmonics as a function of alignment angle

→ amplitude and phase in the wp of the cation

Probing ultrafast electronic dynamics in C_{60} by varying the CEP phase of a short 4fs 720 nm IR pulse

Li et al, *PRL* **2015**, *114*, 123004

Linear polarization (CEP=0) Circular polarization (CEP=0)

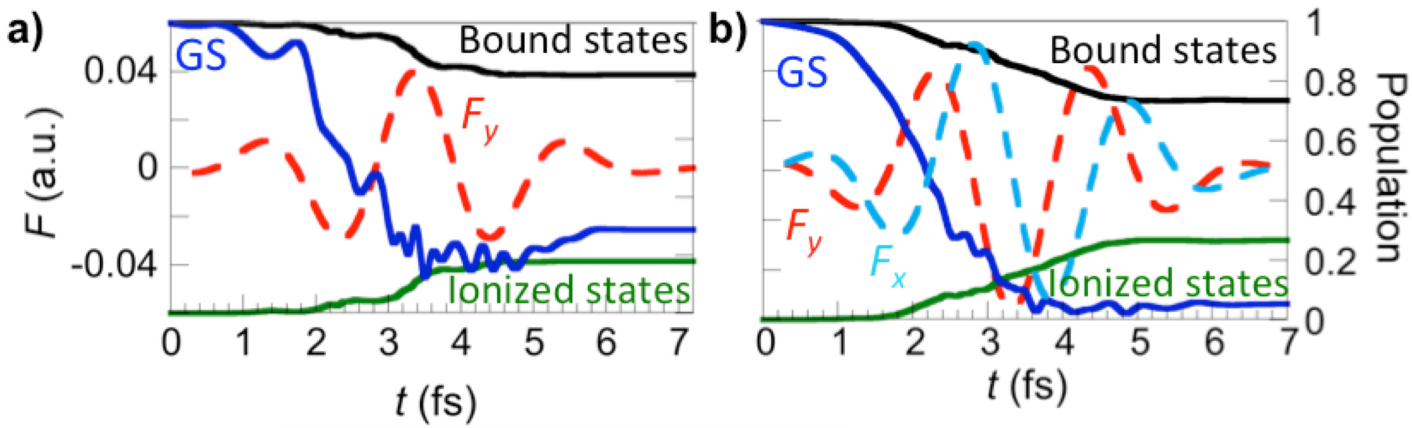

Experiments
MPQ
Matthias Kling
Hui Li

TD-DFT :
CAM-B3LYP/
6-31(+)G(d)
Bq(6 31(6+)G(d))

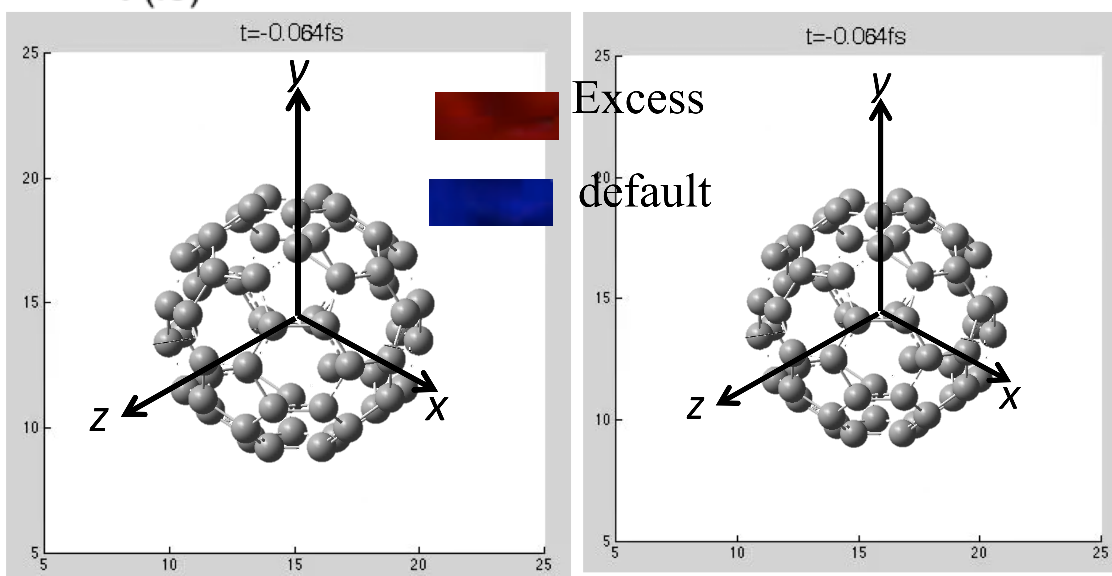

electronic dynamics :
band of 400 states below the IP.

B. Mignolet et al, CPC , **14**, 3332 (2013)

See also *J. Phys. Chem. Lett.* **2016**, *7*, 4677-4682 for the role of SAMO states in SFI of C_{60} and *Scientific Reports* **2017**, *7*, 121 for a study of the photoionization of HoN3@C_{80}.

Probing ultrafast electronic dynamics in C_{60} by varying the CEP phase of a short 4fs 720 nm IR pulse

Hi, Mignolet et al, *PRL* **2015**, *114*, 123004

Experiments
MPQ
Matthias Kling
Hui Li

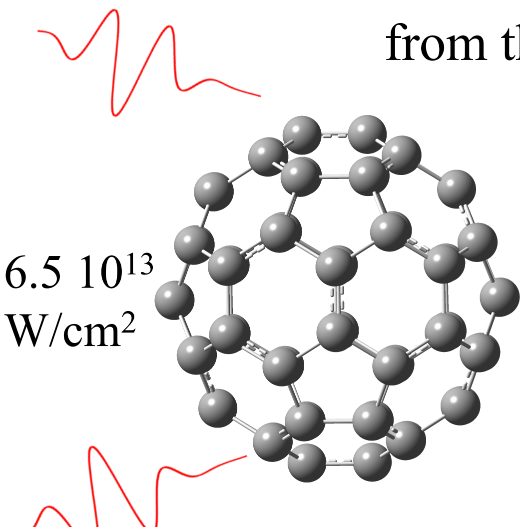

6.5 10^{13} W/cm^2

$$\mathbf{E}(t) = \mathbf{E}\ f(t)\cos(\omega t + \phi_{CEP})$$

CEP=0

Electron ionized from the bottom

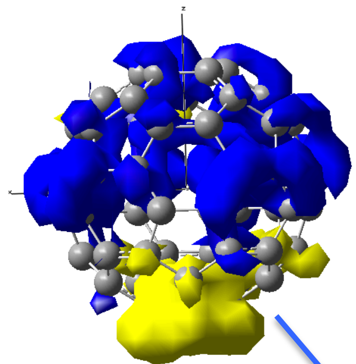

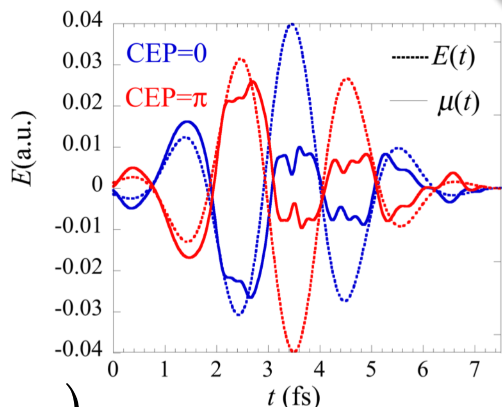

$$A(\mathbf{p}, CEP) = \frac{N_{+y}(\mathbf{p}, CEP) - N_{-y}(\mathbf{p}, CEP)}{N_{+y}(\mathbf{p}, CEP) + N_{-y}(\mathbf{p}, CEP)}$$

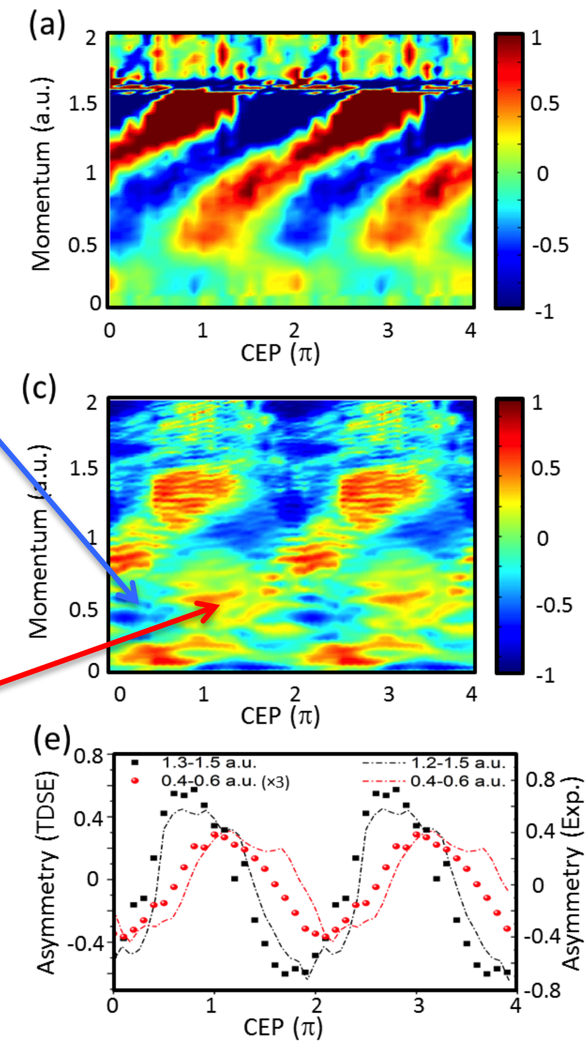

CEP=π

Electron ionized from the top

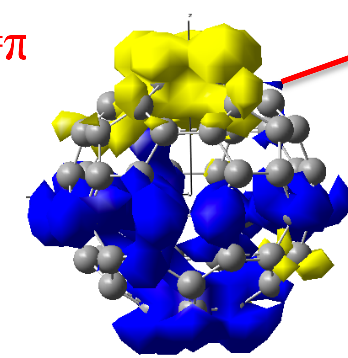

Accumulation of density

Depletion of density

Photoinduced charge migration and charge transfer in small functionalized gold clusters

$Au_{20}(SCH_3)_{15}$bipy
"Au20long"

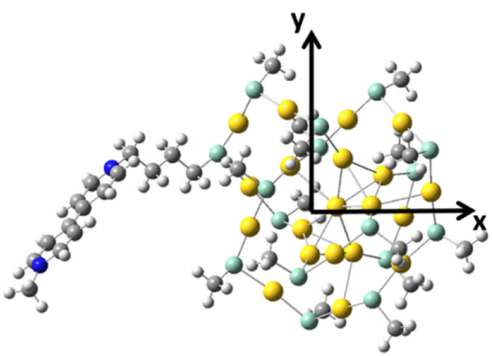

$Au_{11}(PH_3)_7Cl_2$bipy
"Au11 short"

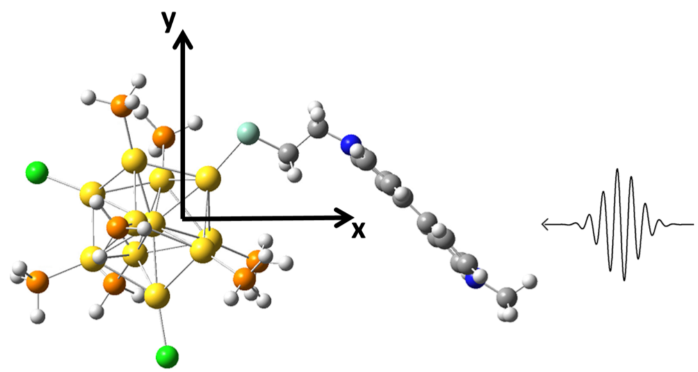

$f_0 = 0.005$ a.u. (8.75 W/cm^2)
$\sigma = 2.8$fs
$\phi = 0$
$\omega_{Au_{11}} = 275$ nm

During excitation

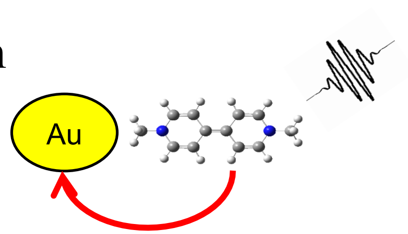

charge transfer

After the pulse

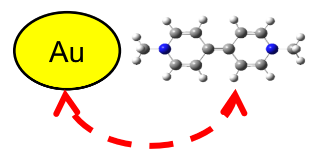

coherent charge migration

QM/MM Equilibrium geometry for the full ligand shell + chromophore : $Au_{11}(Pph_3)_7Cl_2$bipy and Au_{20}(SPh-*t*-but)$_{16}$bipy.

V. Schwanen, F. Remacle
Nanoletters, 2017, *Nano Lett* **17:** 5672-5681

TD-DFT UV-Vis absorption spectra

$Au_{11}(PH_3)_7Cl_2bipy$
"Au11short"

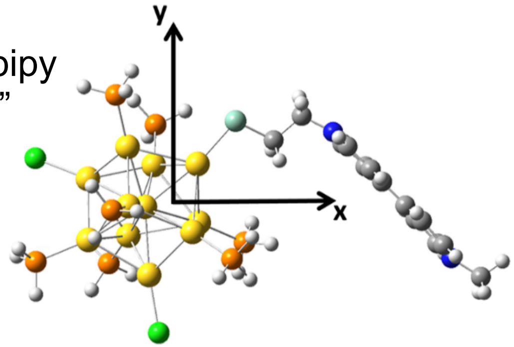

$Au_{20}(SCH_3)_{15}bipy$
"Au20long"

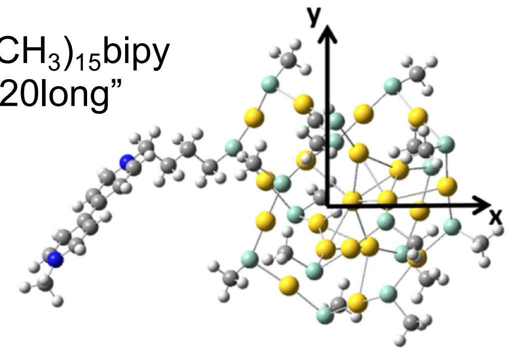

optically active - local on gold
CT bipy to gold

optically active local π-π^* bipy
CT bipy to gold

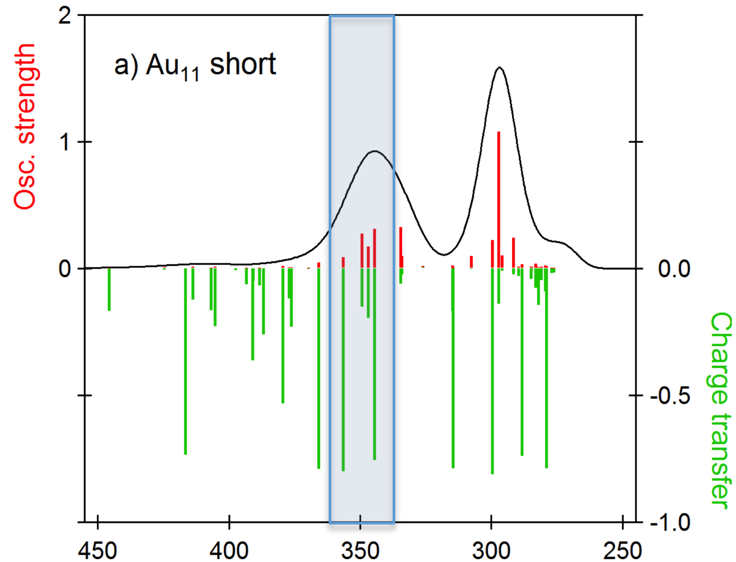

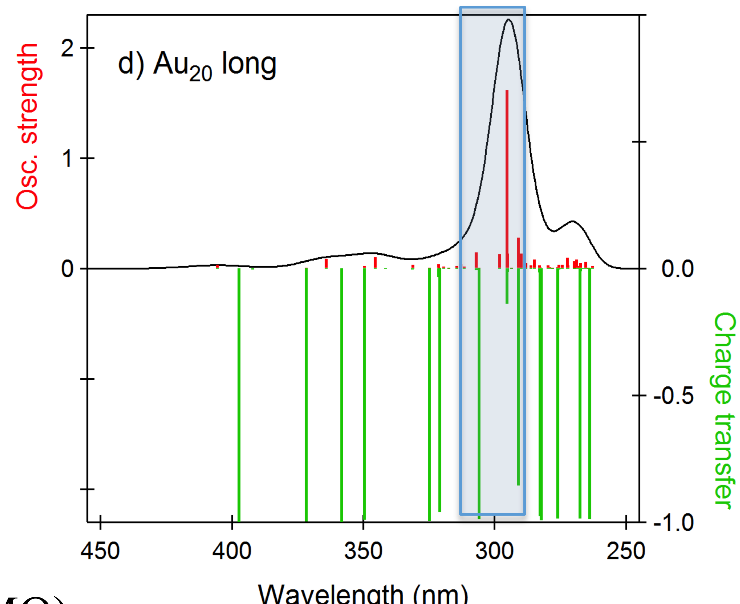

higher intensity of first band (local excitation of SAMO)

TD-DFT CAM-B3LYP tuned with 80% HF exchange

Au : LANL2DZ, C, O, P, Cl, H: 6-31G(d)

Charge transfer and charge migration

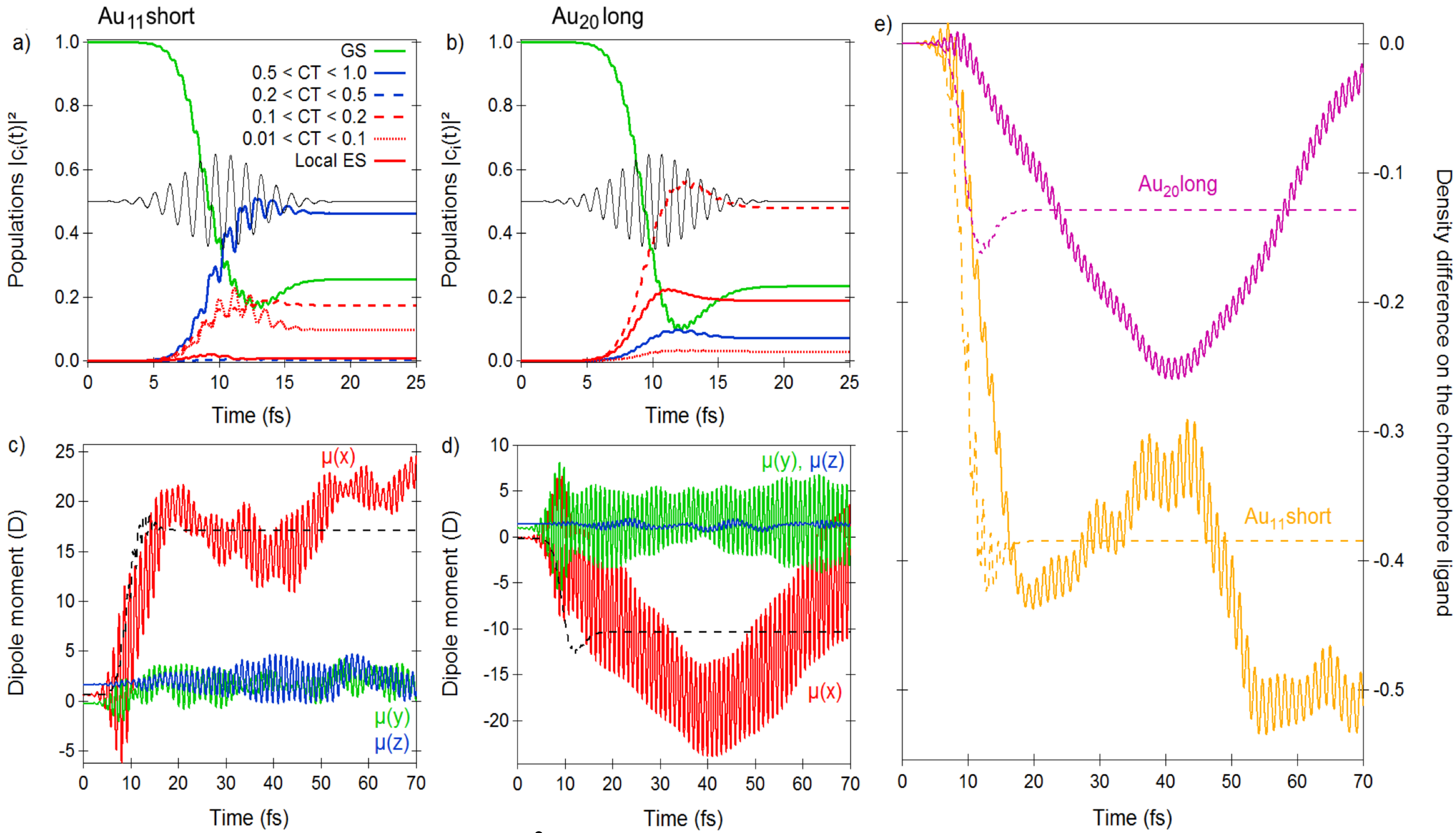

Pulse $f_0 = 0.005$ a.u. (8.75 W/cm^2)

$\omega_{Au_{11}} = 350$ nm

(3.5 eV)

first band

$\phi = 0$

$\sigma = 2.8$ fs

Width $\approx$ 0.8 eV

$\omega_{Au_{20}} = 300$ nm

(4.3 eV)

second band

$$\rho_{diff}^{chr}(t) = \sum_i |c_i(0)|^2 \left[\rho_{ii}^{chr} - \rho_{GS}^{chr}\right]$$

$$+\sum_i \sum_{j \neq i} c_i^*(0) c_j(0) \exp\left(\frac{-i(E_j - E_i)t}{\hbar}\right) \rho_{ij}^{chr}$$

Charge migration in small functionalized gold clusters

Au_{11} CAS averaged(8,14) for 30 ES

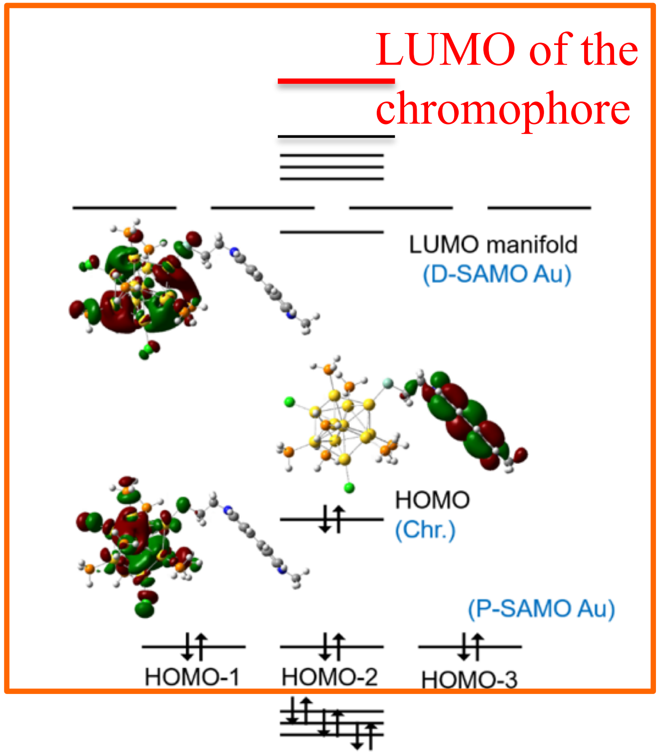

Au : LANL2DZ, C, O, P, Cl, H: 6-31G(d)

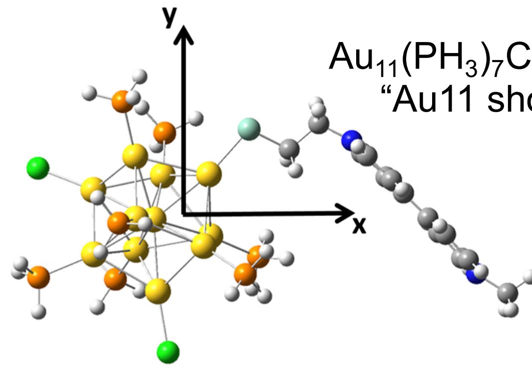

$Au_{11}(PH_3)_7Cl_2bipy$
"Au11 short"

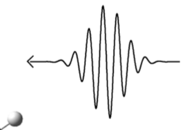

$f_0 = 0.005$ a.u. (8.75 W/cm^2)

$\sigma = 2.8$fs

$\phi = 0$

$\omega_{Au_{11}} = 275$ nm

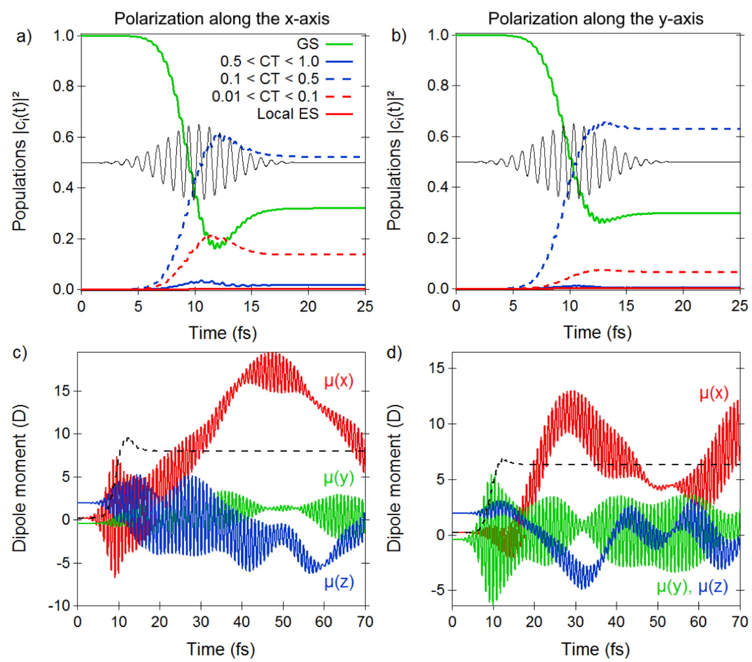

$Au_{11}(PH_3)_7Cl_2bipy$

During excitation

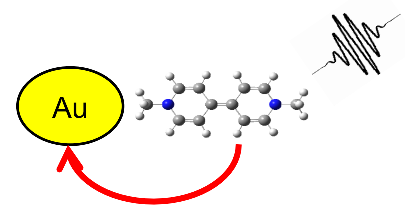

charge transfer

After the pulse

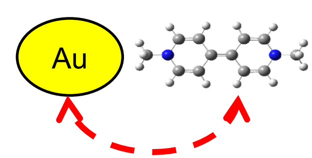

coherent charge migration

V. Schwanen, F. Remacle
2017, *Nano Lett* **17:** 5672-5681

Charge migration in PENNA

Three charge states are involved : the neutral, cation and dication

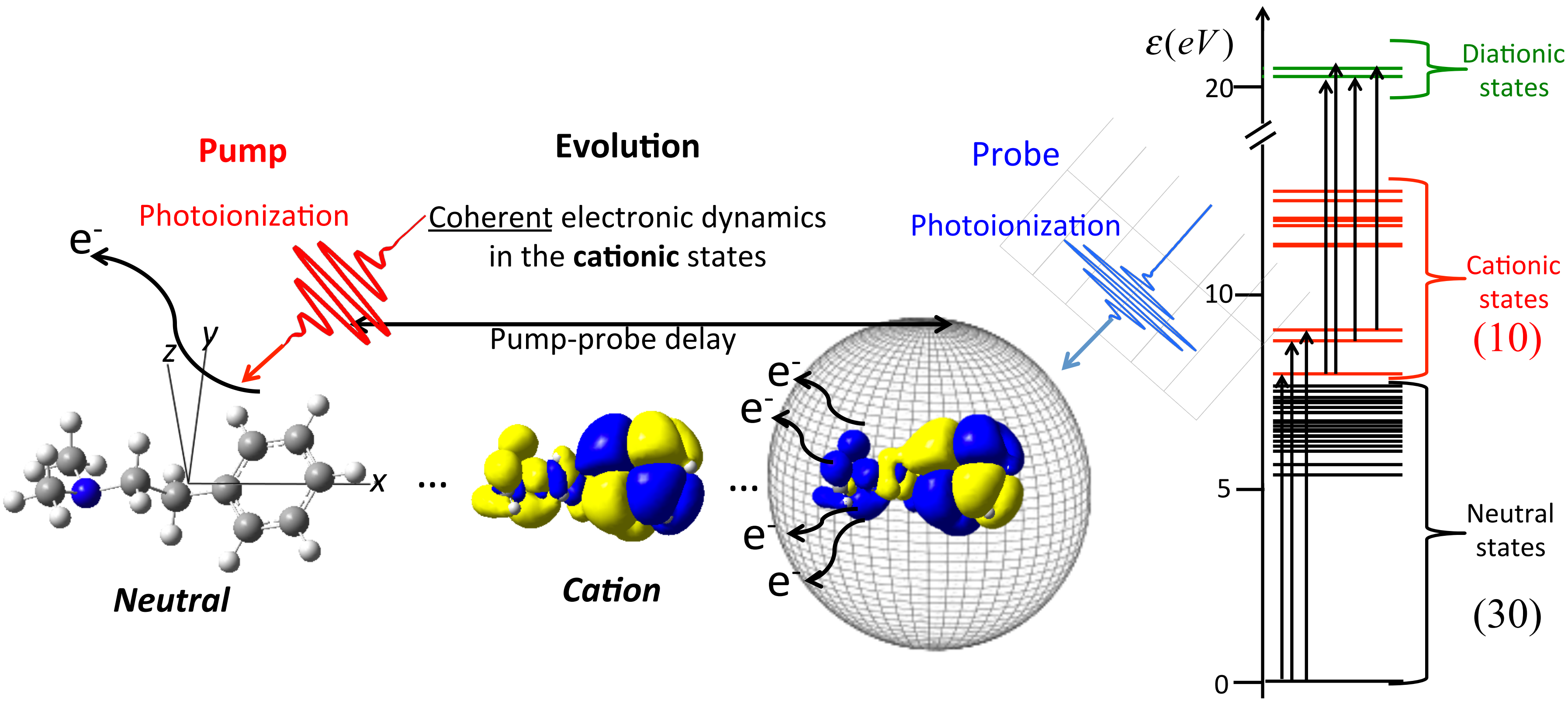

TDDFT : 6–311++ G(d,p) with wB97xD

$$\left|\Psi(t)\right\rangle = \sum_I c_I^{Neut}(t)\left|\Psi_I^{Neut}\right\rangle + \sum_K \sum_{\mathbf{k}_1} c_{K,\mathbf{k}_1}^{Cat}(t)\left|\Psi_K^{cat}, \varepsilon_{\mathbf{k}_1}^{\perp}\right\rangle + \sum_L \sum_{\mathbf{k}_1} \sum_{\mathbf{k}_2} c_{L,\mathbf{k}_1,\mathbf{k}_2}^{Dicat}(t)\left|\Psi_L^{Dicat}, \varepsilon_{\mathbf{k}_1}^{\perp}, \varepsilon_{\mathbf{k}_2}^{\perp}\right\rangle$$

PENNA (surface hopping study in the cation) : S. Sun et al, 2017, *121*, 1442-1447.

IR pump-XUV probe scheme in PENNA

pump : |E| = 0.02 au
polarized along z
probe :: |E| = 0.005 au
polarized along z, ω=13.3 eV

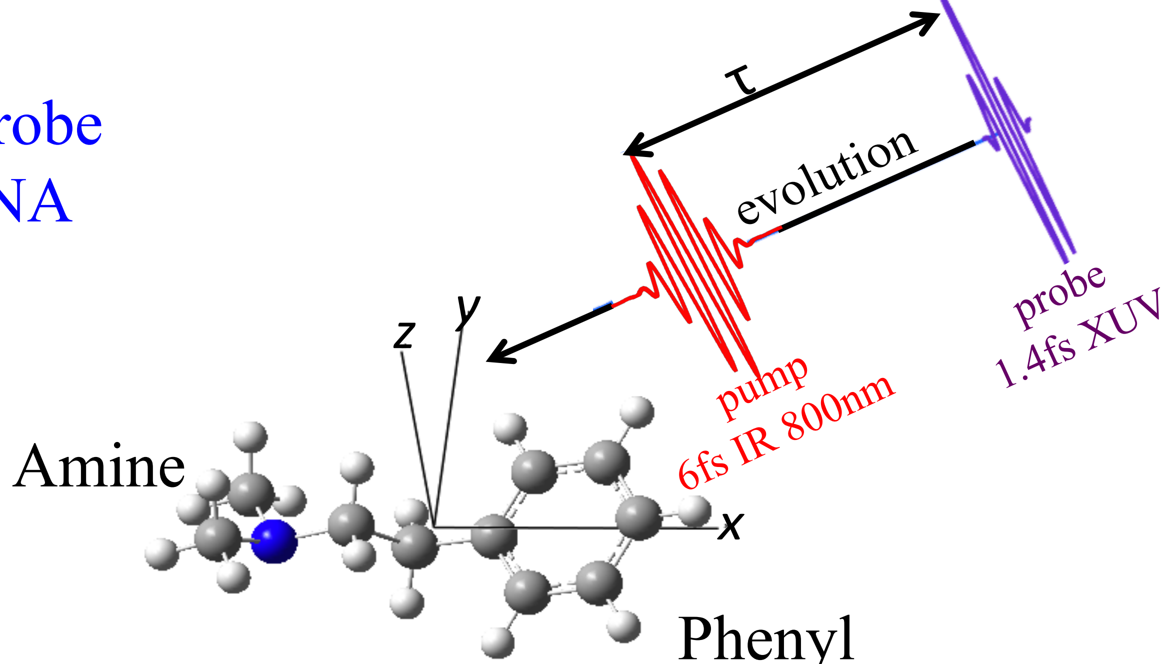

population in the states of the cation

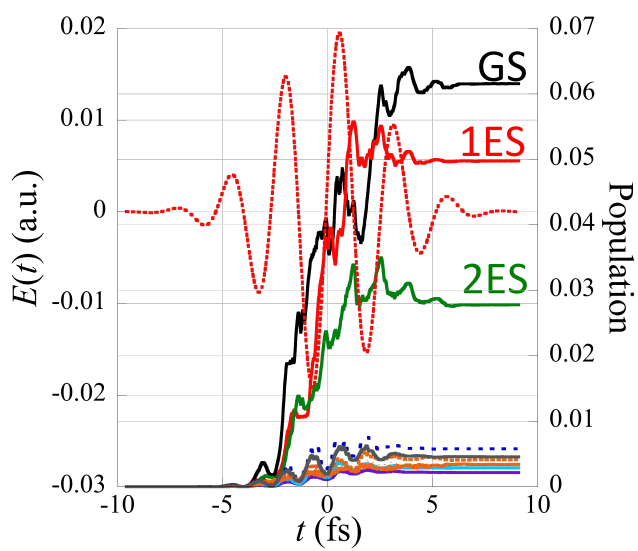

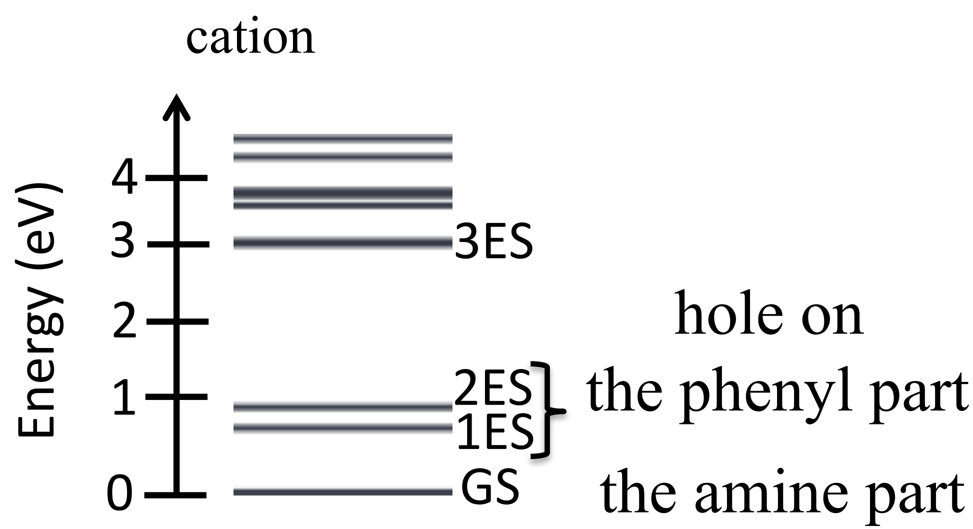

Mignolet, B.; Levine, R. D.; Remacle, F., *J. Phys. B* **2014,** *47*, 124011.

IR pump-XUV probe scheme

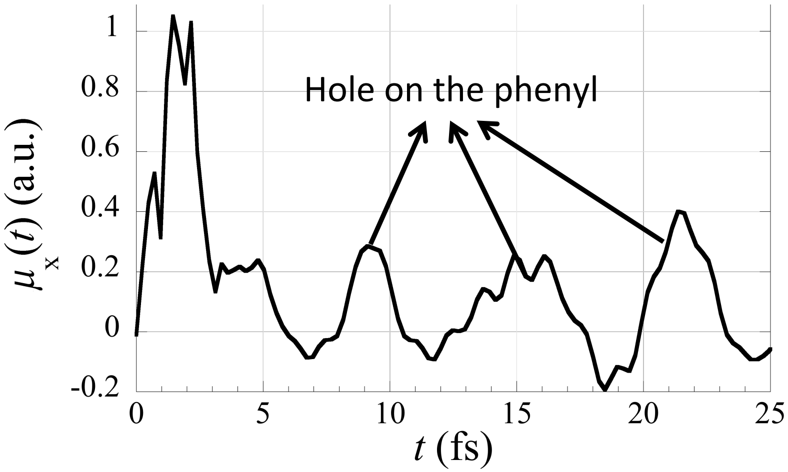

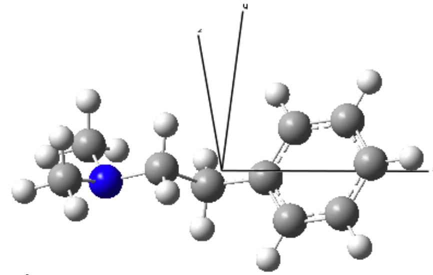

Asymmetry ionization parameter

$$A(\varepsilon,\tau)=\frac{Y_{-x}(\varepsilon,\tau)-Y_{+x}(\varepsilon,\tau)}{Y_{-x}(\varepsilon,\tau)+Y_{+x}(\varepsilon,\tau)}$$

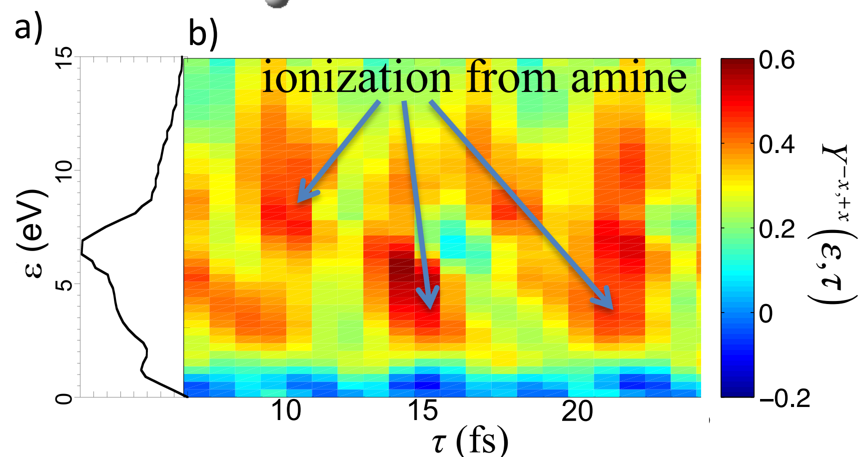

$\rho(t)-\rho(t_0)$ Accumulation of density

Depletion of density

$\mu_x = -0.1$ a.u. $\mu_x = +0.2$ a.u.

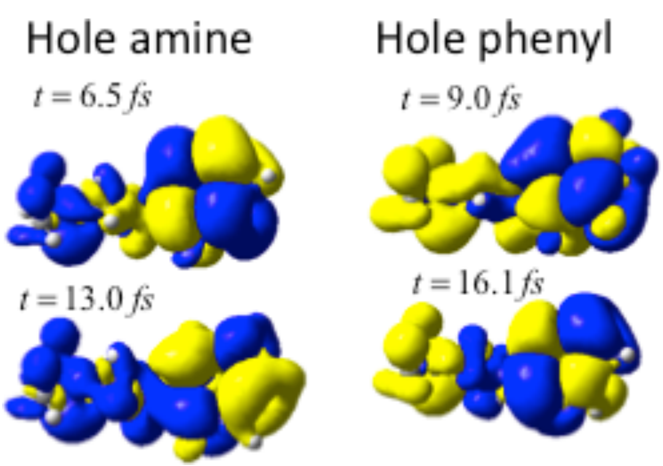

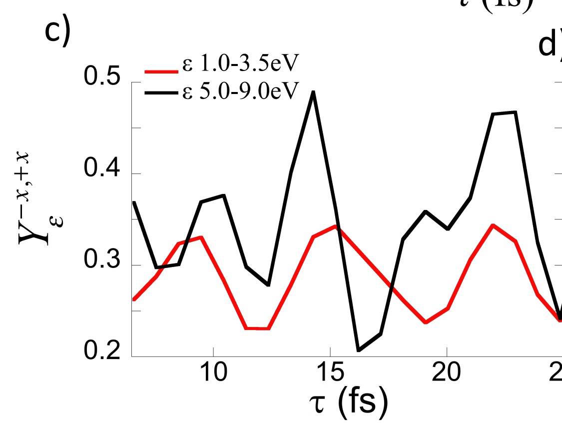

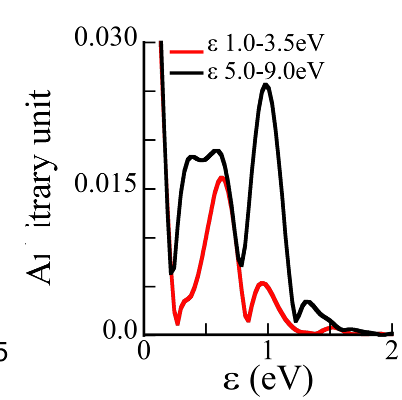

Mignolet, B.; Levine, R. D.; Remacle, F., *J. Phys. B* **2014,** *47*, 124011.

An electronic time scale for chemistry?
Is there a Post Born-Oppenheimer era?

Explore the regime of purely electronic dynamics before the onset of the nuclear motion

Long term :

Can one use ultrafast excitation of electrons out of equilibrium to drive the motion of the nuclei to specific products?

An electronic time scale for chemistry?

Chemical reactions imply a change in the configuration of the nuclei. Therefore the time scale of chemistry is the time for nuclear motion.

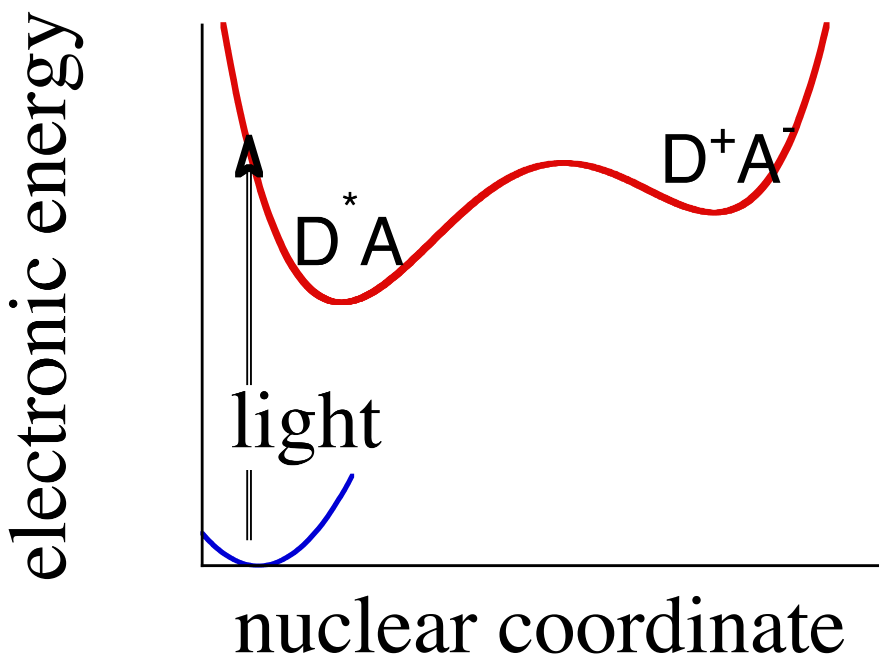

- Born-Oppenheimer separation: The light electrons **instantaneously** adjust to the position of the nuclei.
- Changes in electronic state are induced by motion of the nuclei.

F. Remacle and R. D. Levine,
Proc. Natl. Acad. Sci. USA **103**, 6793 (2006)

Attochemistry is qualitatively different

Photoexcitation
Photoionization → non equilibrium electronic density → NAC in a dense manifold of electronic states

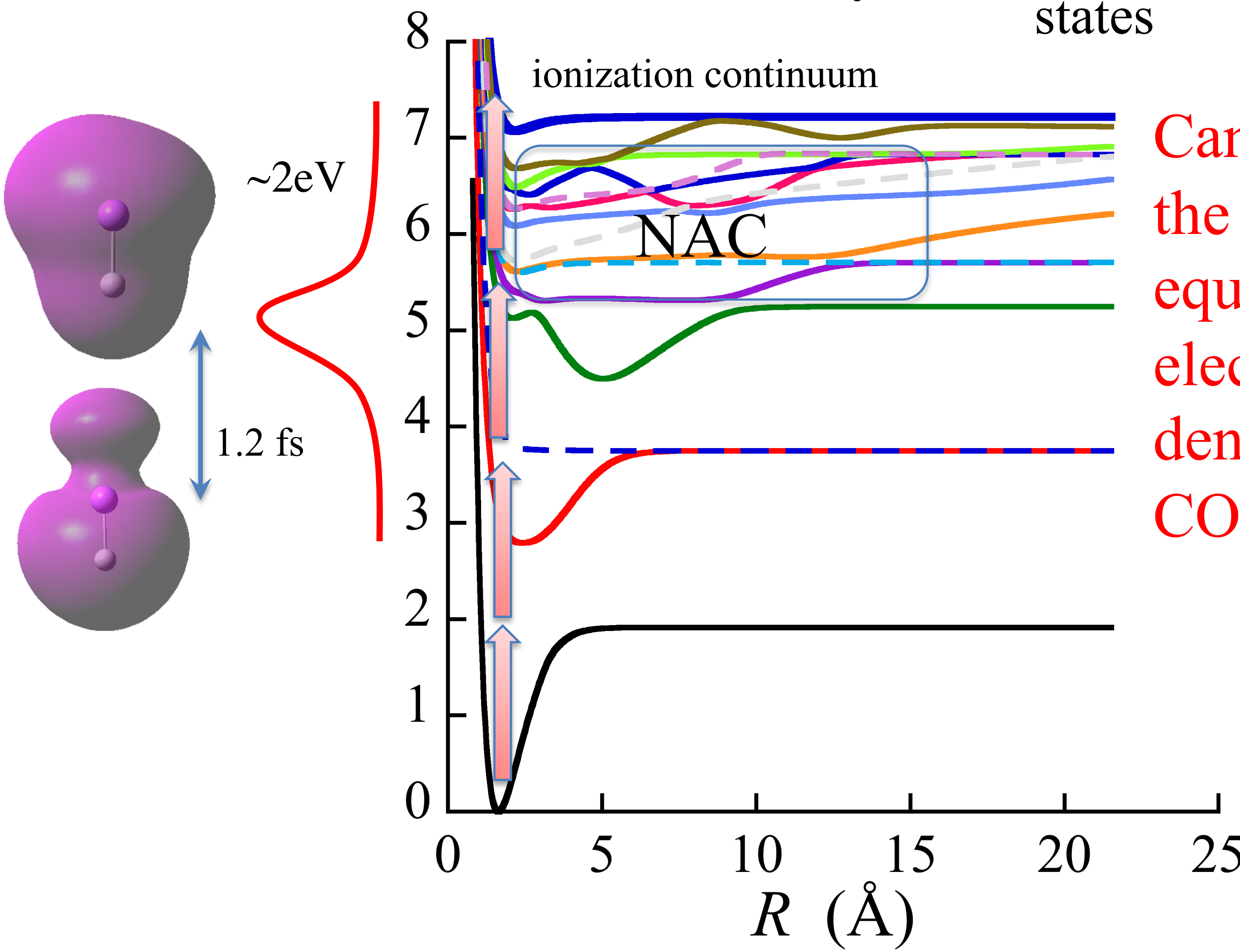

Can we exploit the non equilibrium electronic density for CONTROL ?

Onset of nuclear motion

Several time scales and several electronic states are involved

- Time scale of the electronic motion, atto to few femto seconds
- Dipole coupling to strong fields for all electronic states
- Time scale for the electron-nuclei motion, up to ps
- Non adiabatic coupling induced by nuclear motion

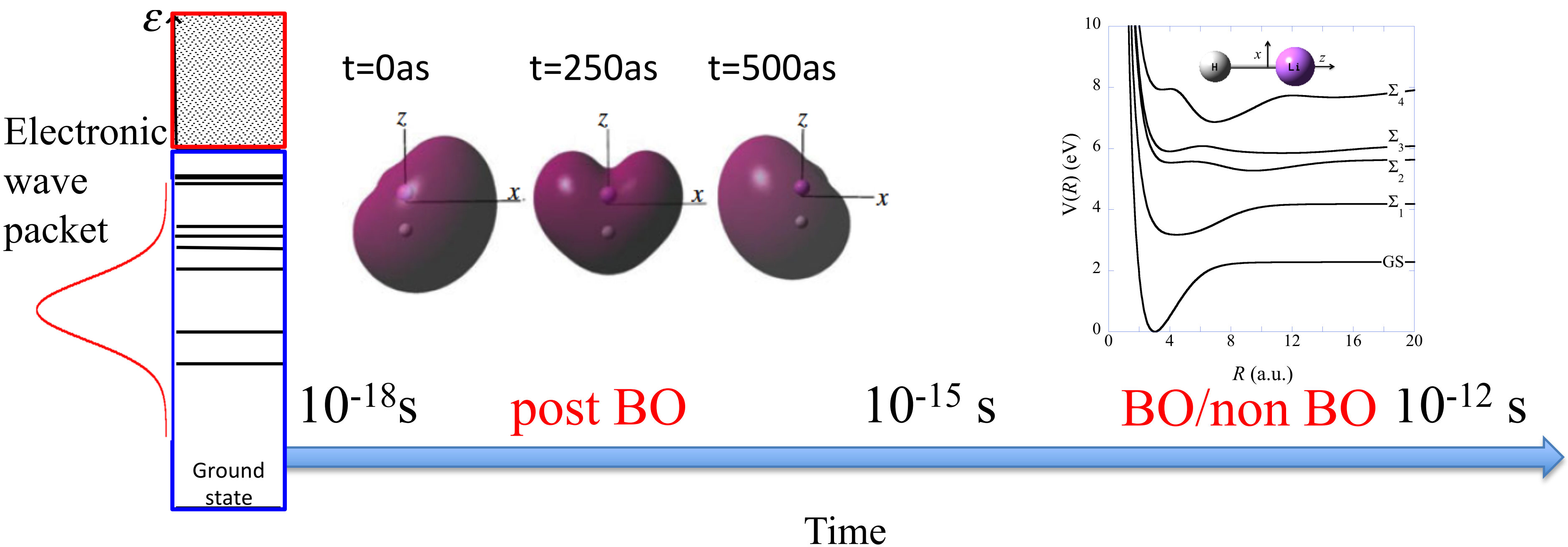

Fully quantal electron-nuclear dynamics

by the time-dependent nuclear Schrodinger equation on a grid

Challenges

- The pulses are short and therefore broad in energy, resulting in the coherent excitation of several electronic states coupled by transient dipoles, non adiabatic couplings (NAC), and photoionisation.
- Several nuclear degrees of freedom are involved, multidimensional grids.

Methodological developments

- Implement a finite difference algorithm for computing momentum and kinetic energy, in several nuclear dimensions.

S. A. Jayantha, K. G. Komarova, S. van den Wildenberg, F. Remacle and R. D. Levine, in *Attosecond Molecular Dynamics*, eds. M. J. J. Vrakking and F. Lepine, Royal Society of Chemistry, Cambridge, 2018, vol. 13, pp. 308-347.

- Efficient methodology for computing the photoionization matrix elements for each set of nuclear coordinates.

S. van den Wildenberg, B. Mignolet, R. D. Levine, F. Remacle, JCP 2019 submitted.

Photoionization is included in the TDSE using the partitioning technique

Two orthogonal subspaces $\mathbf{1} = \mathbf{Q} + \mathbf{P}$

$$\mathbf{Q} = \sum_{i,g}^{N_{neut} N_g} \left| \Psi_i^{neut}(\mathbf{r};\mathbf{R})\theta(\mathbf{R}_g) \right\rangle \left\langle \Psi_i^{neut}(\mathbf{r};\mathbf{R})\theta(\mathbf{R}_g) \right|$$

Neutral bound subspace

$$\mathbf{P} = \sum_{j,g,k}^{N_{cat},N_k} \left| \Psi_j^{cat}(\mathbf{r};R_g)\theta(R_g)\phi_{\mathbf{k}}^{\perp elec}(\mathbf{r}) \right\rangle \left\langle \Psi_j^{cat}(\mathbf{r};R_g)\theta(R_g)\phi_{\mathbf{k}}^{\perp elec}(\mathbf{r}) \right|$$

Continuum subspace

$$\begin{cases} \dfrac{dc_{ig}^{neut}(t)}{dt} = \displaystyle\sum_{i'g'}^{N_{neut},N_g} H_{ig,i'g'}(t)\, c_{i'g'}^{neut}(t) + \sum_{j'g'\mathbf{k}'}^{N_{cat},N_k,N_g} H_{ig,j'g'\mathbf{k}'}(t)\, c_{j'g'\mathbf{k}'}^{cat}(t) \\ \dfrac{dc_{jg\mathbf{k}}^{cat}(t)}{dt} = \displaystyle\sum_{i'g'}^{N_{neut},N_g} H_{jg\mathbf{k},i'g'}(t)\, c_{i'g'}^{neut}(t) + \sum_{j'g'\mathbf{k}'}^{N_{cat},N_k,N_g} H_{jg\mathbf{k},j'g'\mathbf{k}'}(t)\, c_{j'g'\mathbf{k}'}^{cat}(t) \end{cases}$$

Total nuclear wave function

$$\Phi(R_g,t) = \sum_{ig}^{N_{neut},N_g} c_{ig}^{neut}(t)\theta(R_g) + \sum_{jg\mathbf{k}}^{N_{cat},N_k,N_g} c_{jg\mathbf{k}}^{cat}(t)\theta(R_g)$$

Matrix elements

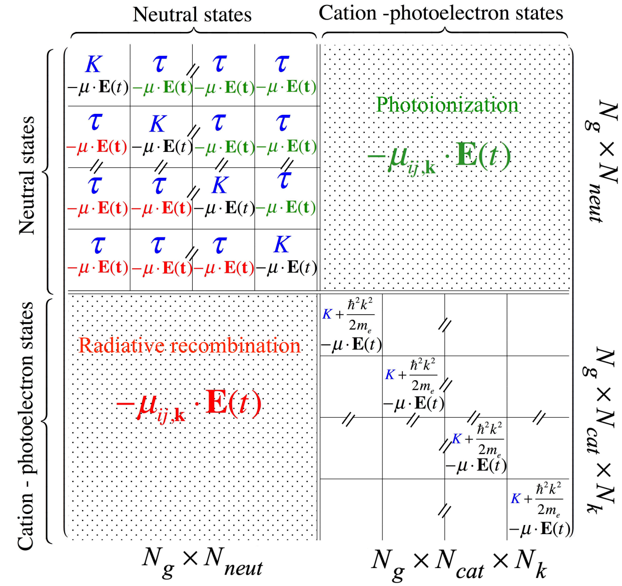

Bound subspace

$$H_{ig,jg'}(R,t)=\left(-\frac{\hbar^2}{2\mu}\nabla_R^2\right)_{g,g'}\delta_{ij}+V_{ig,jg'}(R)\delta_{ij}\delta_{gg'}$$

$$-\mathbf{E}(t)\left(\mu^{elec}_{ig,jg'}(R)+\mu^{nucl}_{gg'}(R)\delta_{ij}\right)\delta_{gg'}$$

Photoexcitation + AC Stark shift

$$-\frac{\hbar^2}{2\mu_{\text{LiH}}}\left(2\tau_{ij}\left(R_g\right)\left(\nabla_R\right)_{gg'}+\sum_l\tau_{il}\left(R\right)\tau_{lj}\left(R\right)\delta_{gg'}+g_{ij}\left(R\right)\delta_{gg'}\right)$$

NAC

Continuum

$$\hat{H}=\hat{T}_{nucl}+\hat{H}^{elec}_{cat}+-\frac{1}{2}\hat{\nabla}_l^2-\mathbf{E}(t).\mathbf{r}_l$$

$$H_{jg\mathbf{k},j'g'\mathbf{k}'}(t)=-\frac{\hbar^2}{2\mu_{LiH}}(\nabla^2)_{gg'}\delta_{jj'}+V_j(R)\delta_{jg,j'g'}-\vec{E}(t)\cdot(\mu_{jj}(R)\delta_{jj'}+\mu_{jj'}(R))\delta_{gg'}+\frac{[\hbar\mathbf{k}+eA(t)]^2}{2m_e}\delta_{\mathbf{kk}'}$$

AC ‘Stark’ shift

Photoionization matrix elements

$$H_{ig,jg'\mathbf{k}}=-\mathbf{E}(t)\left\langle\phi^{Dyson}_{ij'}\left(\mathbf{r};R_{g'}\right)\middle|\mathbf{r}\middle|\phi^{\perp elec}_{\mathbf{k}}\right\rangle\delta_{g'g}$$

$\left|\phi^{\perp elec}_{\mathbf{k}}\right\rangle$ orthogonalized plane waves

$$\phi^{Dyson}\left(\mathbf{r}\right)=\left\langle\Phi_{cat}\middle|\Phi_{neut}\right\rangle=\sum_i d_i\phi_i^{MO}\left(\mathbf{r}\right)\qquad\phi_i^{MO}\left(\mathbf{r}\right)=\sum_j c_{ji}\chi_j^{AO}\left(\mathbf{r}\right)$$

Control of fragmentation yields in LiH through the carrier envelope phase including photoionization

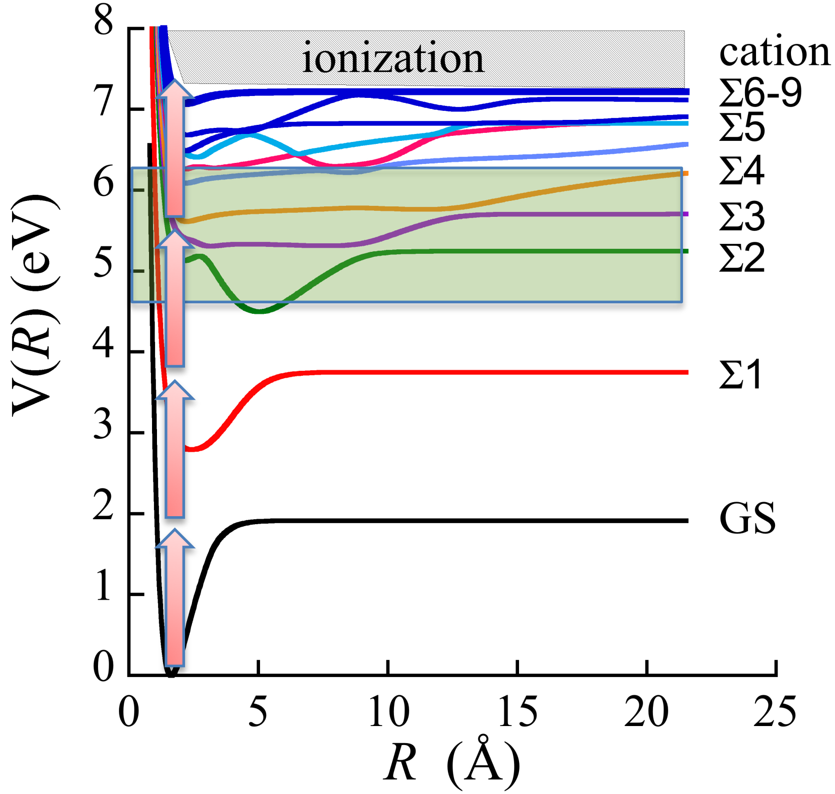

Dipole

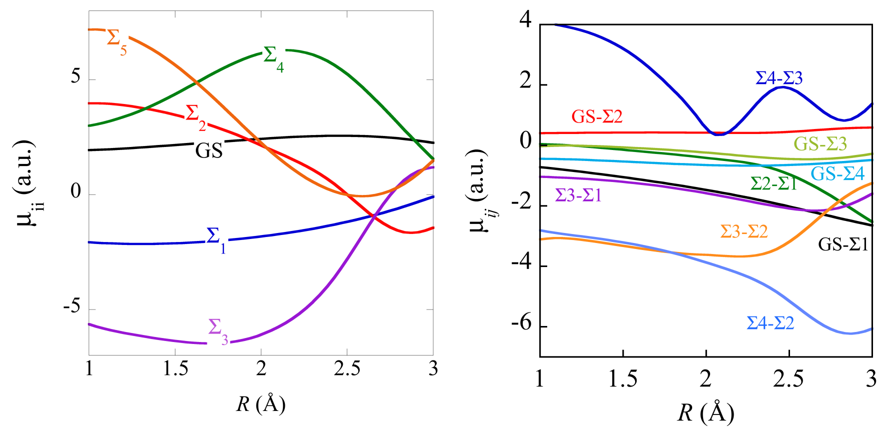

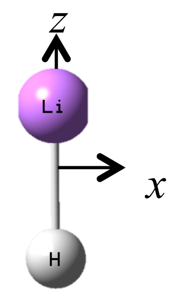

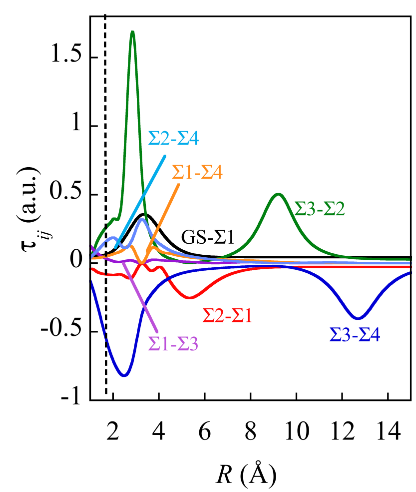

NAC

256 grid points per electronic state

28672 discretized states of the continuum per grid points

= 7.3 10^6 coefficients

S. van den Wildenberg, B. Mignolet, R. D. Levine, F. Remacle, 2019, JCP submitted

SA18-CASSCF(4,20) / 6-311++G(3df,3dp) + S and P Rydberg, SA4-CAS for the cation

CEP control of the populations at the end of the pulse

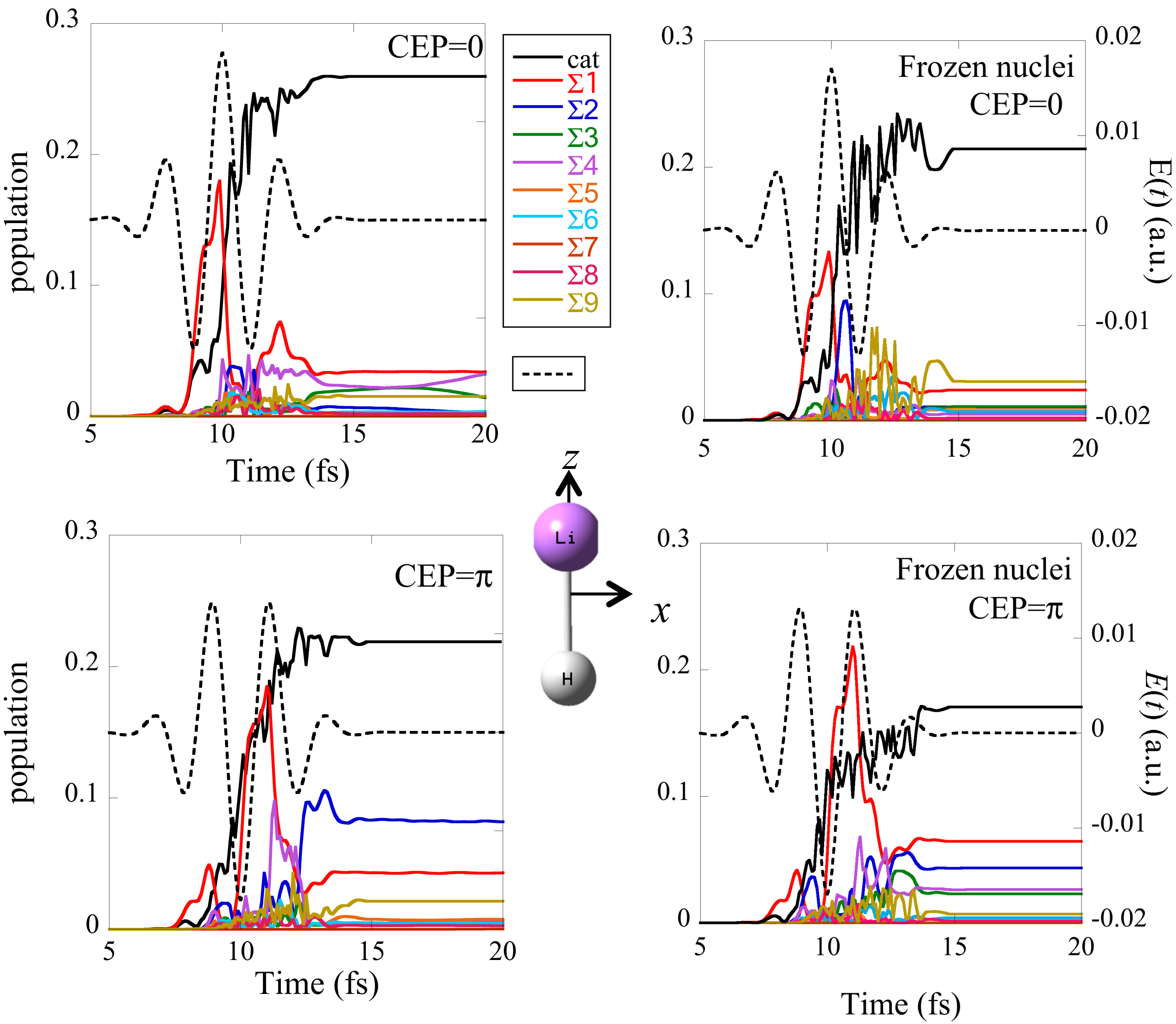

	CEP=0	
t= 15 fs	Nuc mot	Req
GS	0.635	0.687
$\sum_1$	0.034	0.024
$\sum_2$	0.007	0.011
$\sum_3$	0.020	0.011
$\sum_4$	0.023	0.005
$\sum_5$	0.001	0.009
cat	0.259	0.214

	CEP=π	
GS	0.608	0.665
$\sum_1$	0.043	0.065
$\sum_2$	0.083	0.043
$\sum_3$	0.004	0.023
$\sum_4$	0.004	0.026
$\sum_5$	0.008	0.003
cat	0.219	0.17

Pulse parameters : ω=0.063 au (1.17 eV, 720 nm)
$|E_z|$=0.01 au (1 10^{13}W/cm^2), FWHM=3.5 fs

Correlation between the dipole moments of the neutral and that of the photoelectron during the pulse

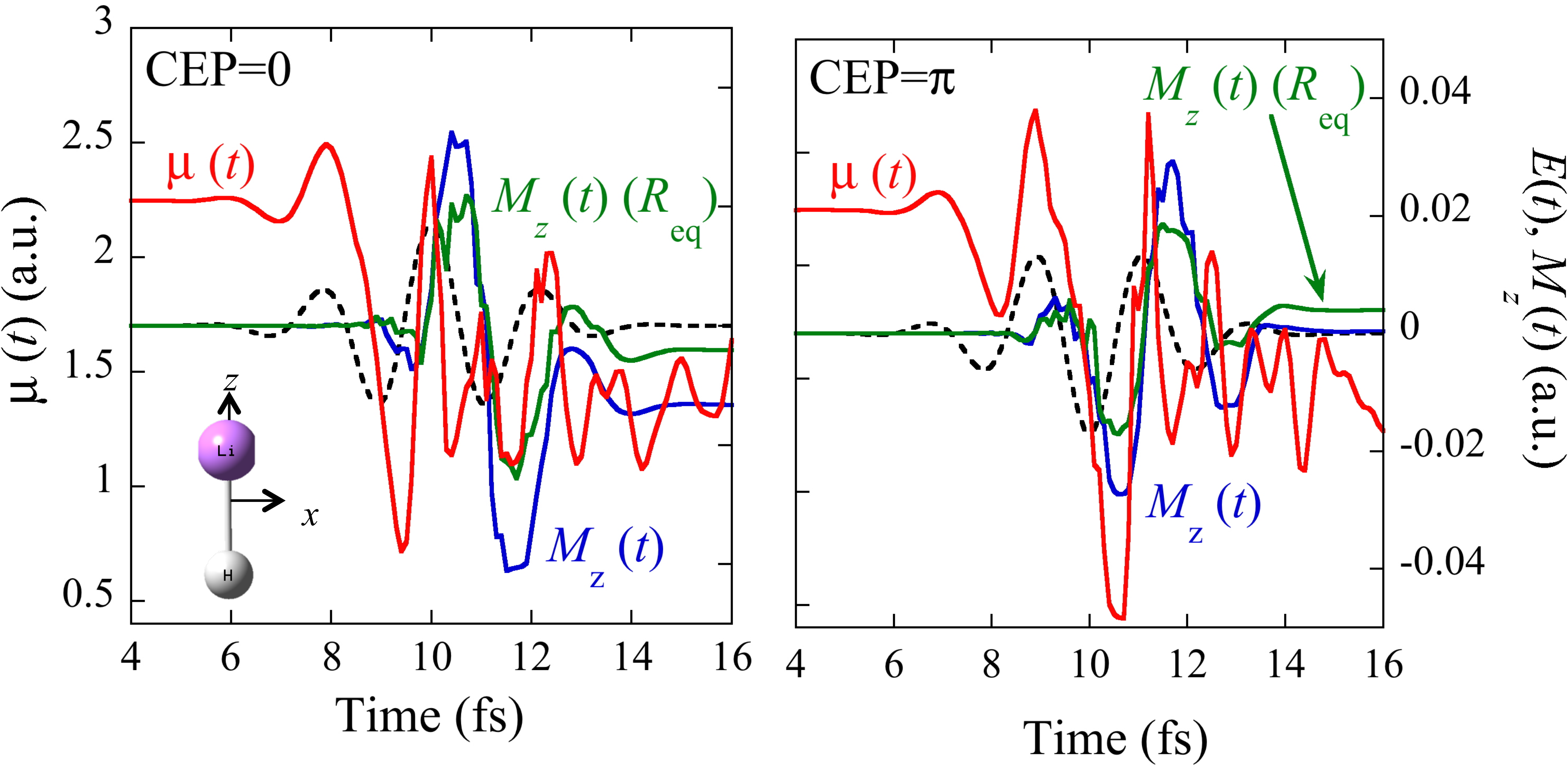

$$\mu(t) = \langle \Psi(t)\mathbf{Q} | \hat{\mu} | \mathbf{Q}\Psi(t) \rangle = \sum_{i,i'}^{N_e} \sum_{g}^{Ng} c_{ig}^{*}(t) c_{i'g}(t) \mu_{ii'}(R_g)$$

$$M_z(t) = -|e| \langle p_z(t) \rangle = -|e| \hbar \sum_{|k|,\Omega}^{N_k} \rho(|k|) d|k| d\Omega \left| c_{g,|k|,\Omega}(t) \right|^2 k_z$$

Correlation of the localization in space and in time of the densities of the neutral and the photoelectron during the pulse

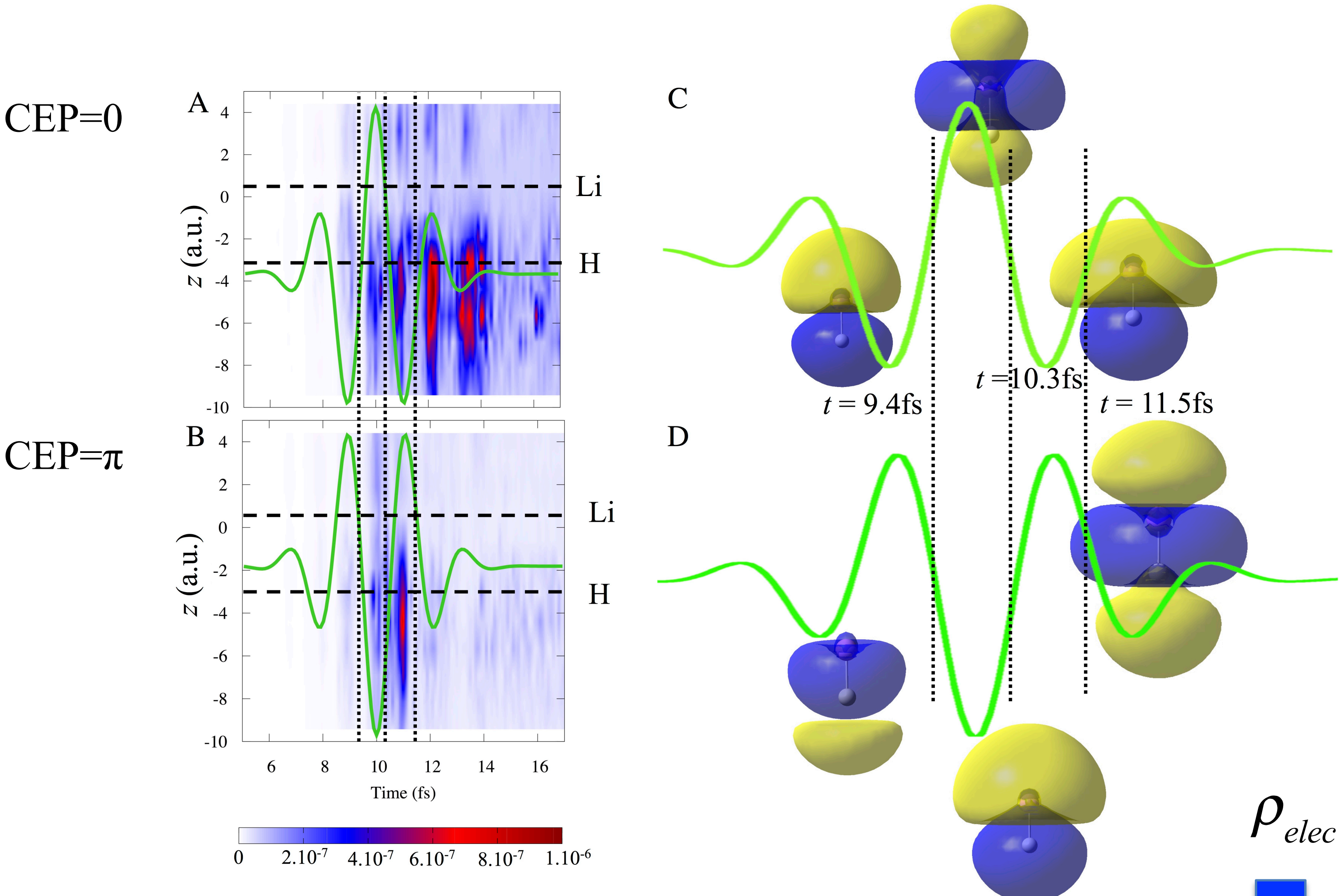

$$\rho_{elec}(t) - \rho_{GS}$$

defect

excess

$$\left|\Psi_{elec}(z,t)\right|^2 = \sum_{x,y} dxdy \left| \sum_{|k|,\omega} \rho(|k|) d|k| d\Omega c_{|k|,\Omega}(t) \phi_{\mathbf{k}}^{\perp,elec}(x,y,z) \right|^2$$

CEP control is maintained when the vibronic WP goes through NAC regions

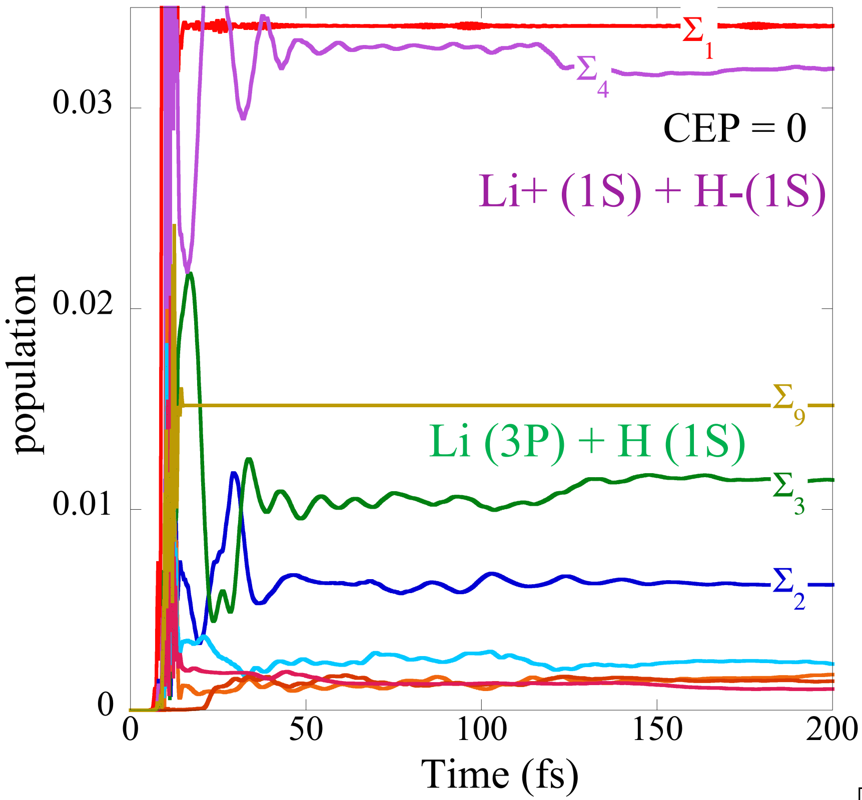

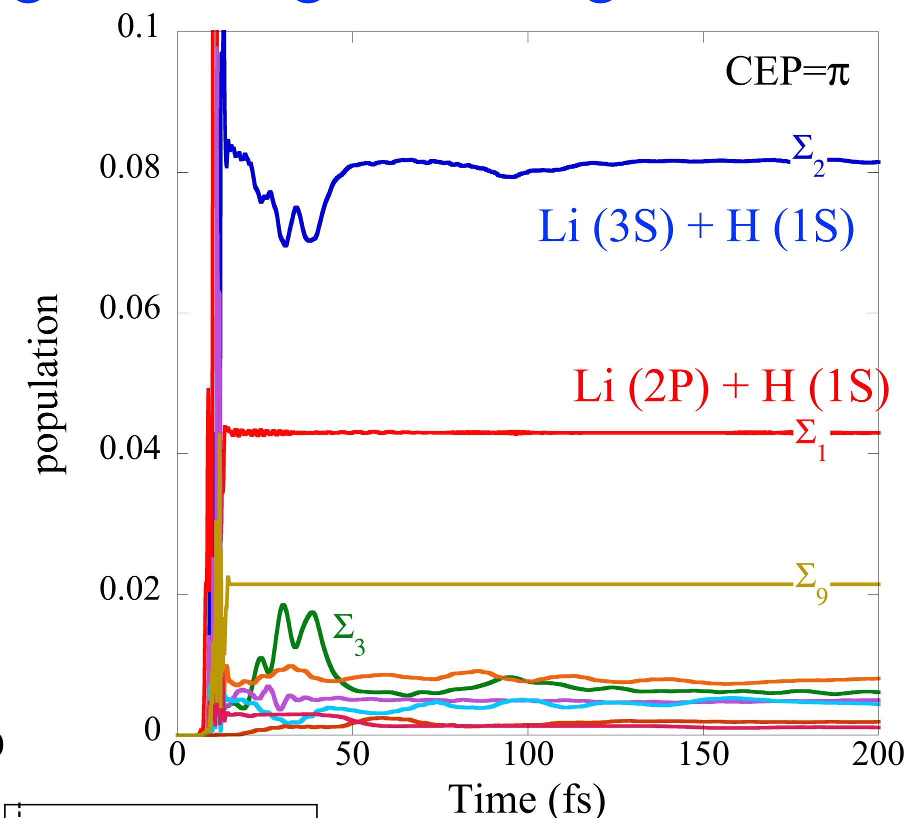

$t = 200$ fs $\quad \Sigma_1 \simeq \Sigma_4 > \Sigma_3 > \Sigma_2$

0.034 0.032 0.011 0.0062

$t = 200$ fs $\quad \Sigma_2 > \Sigma_1 > \Sigma_3 \approx \Sigma_4$

0.08 0.043 0.006

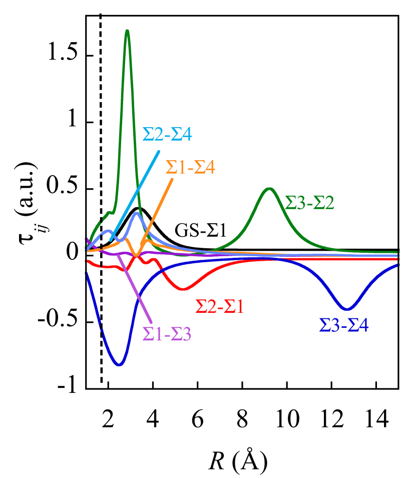

NAC

S. van den Wildenberg, B. Mignolet, R. D. Levine, F. Remacle, JCP 2019 submitted.

See also A. Nikodem, R. D. Levine and F. Remacle, *Phys. Rev. A*, 2017, **95**, 053404.

Oscillations of the time-dependent dipole reflect the CEP

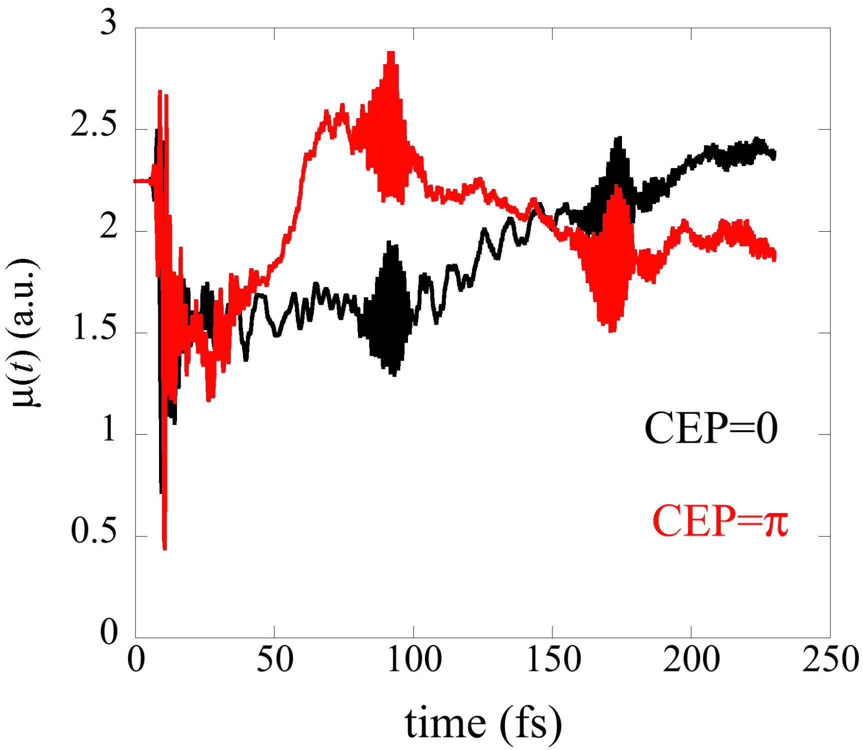

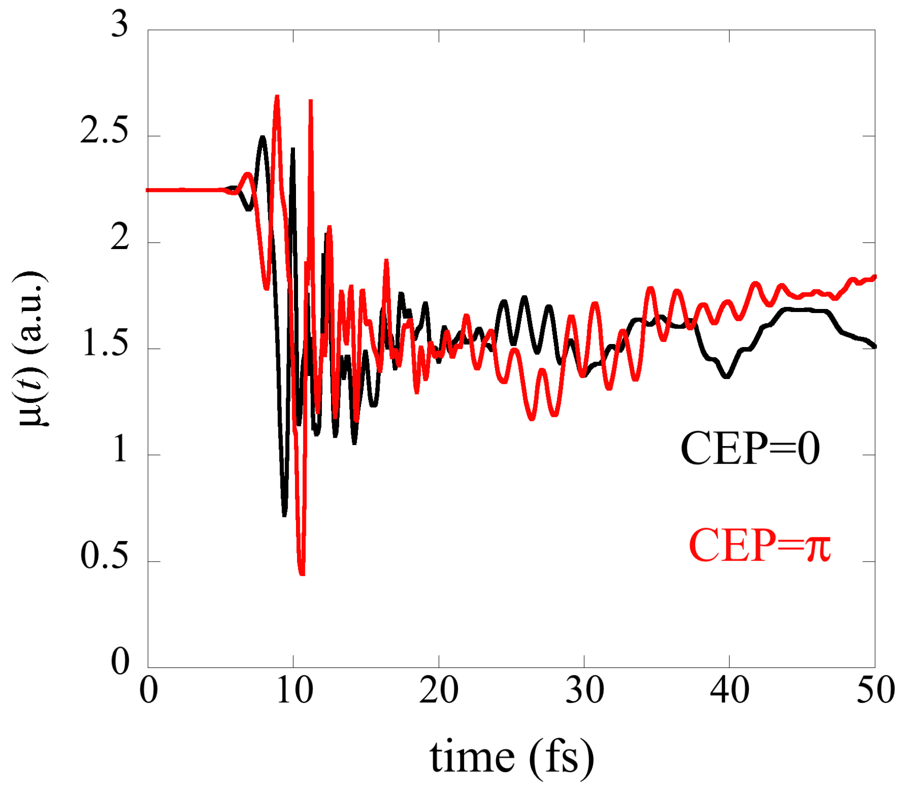

CEP is imprinted on the phase of the coherence in space and in time in spite of photoionization and strong NAC coupling

$$2\,\mathrm{Re}\left[c^{*}_{\Sigma 2,g}(t)\,c_{\Sigma 3,g}(t)\right]$$

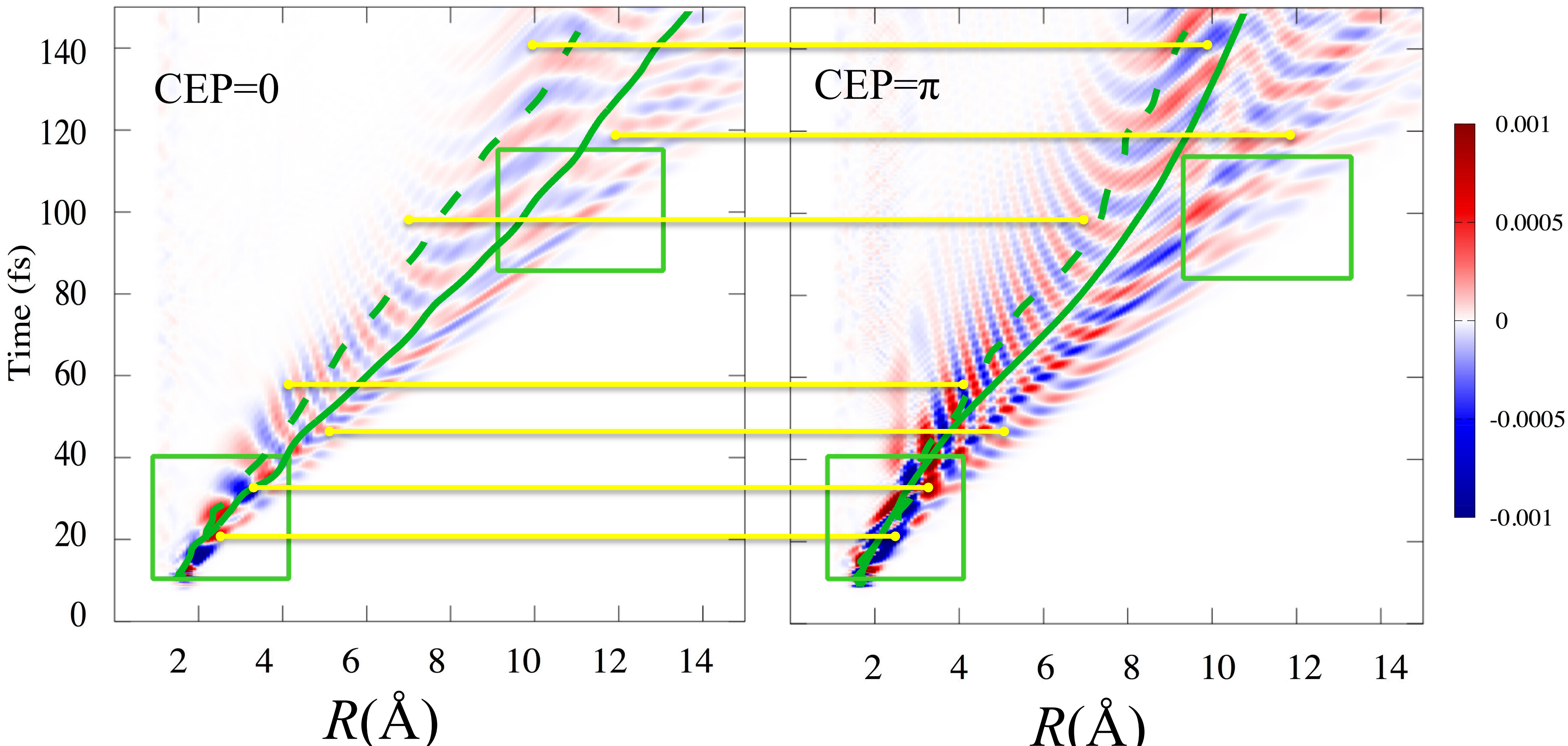

- CEP control: WP's on Σ_2 and Σ_3 travel and delocalize differently
- First NAC : the Σ_2–$\Sigma_3$coherences are out of phase for CEP=0 and CEP=π
- WP's travel faster for CEP = 0
- Before the second NAC region : two branches
  - Lower branch : Σ_2–Σ_3 coherences remain out of phase
  - Upper branch : in phase

Electronic coherence and populations through the first NAC region

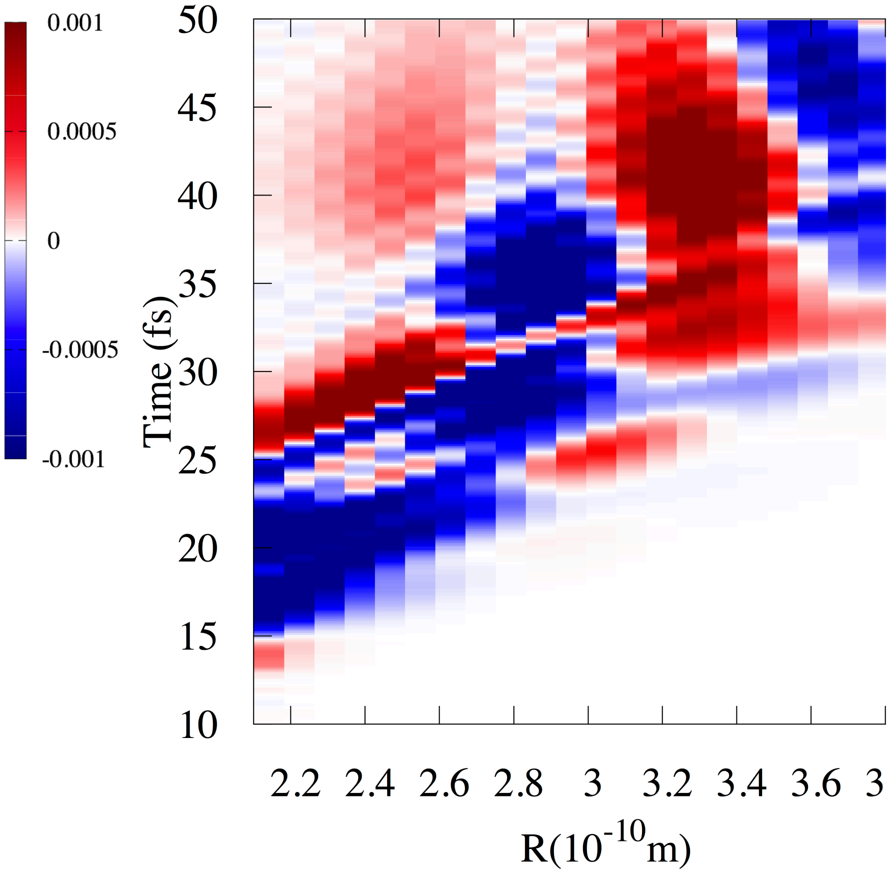

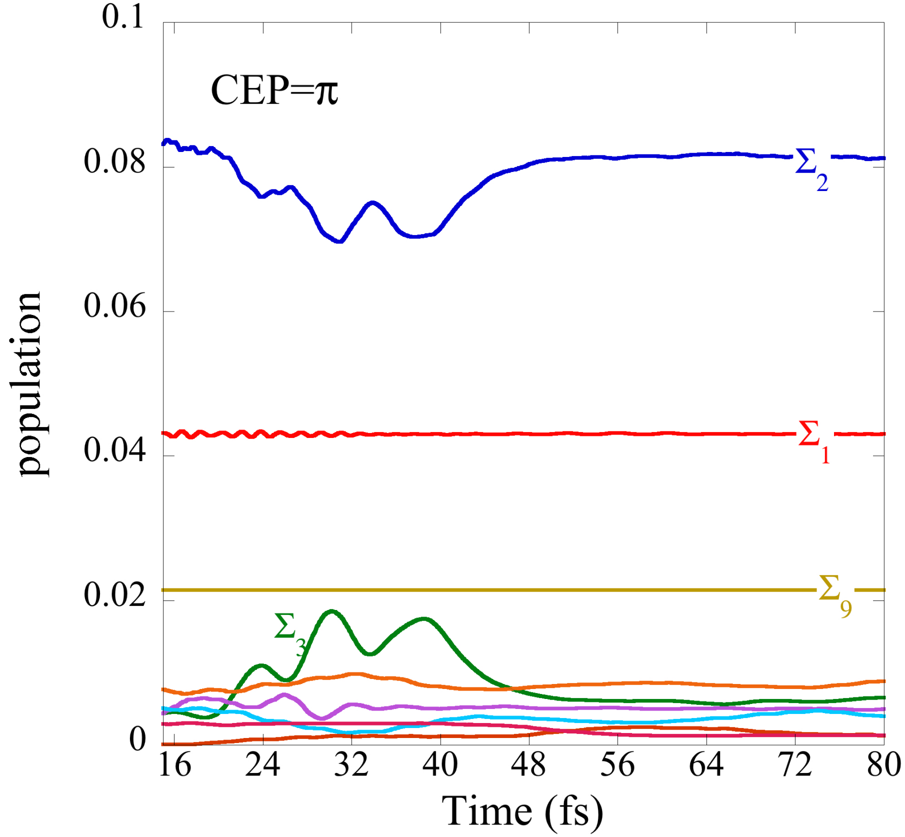

Period of 6.5-8 fs going through the NAC region

Isocontours of the the non equilibrium electronic density, $\rho_{elec}(\mathbf{r},t;R)$ through the first NAC region

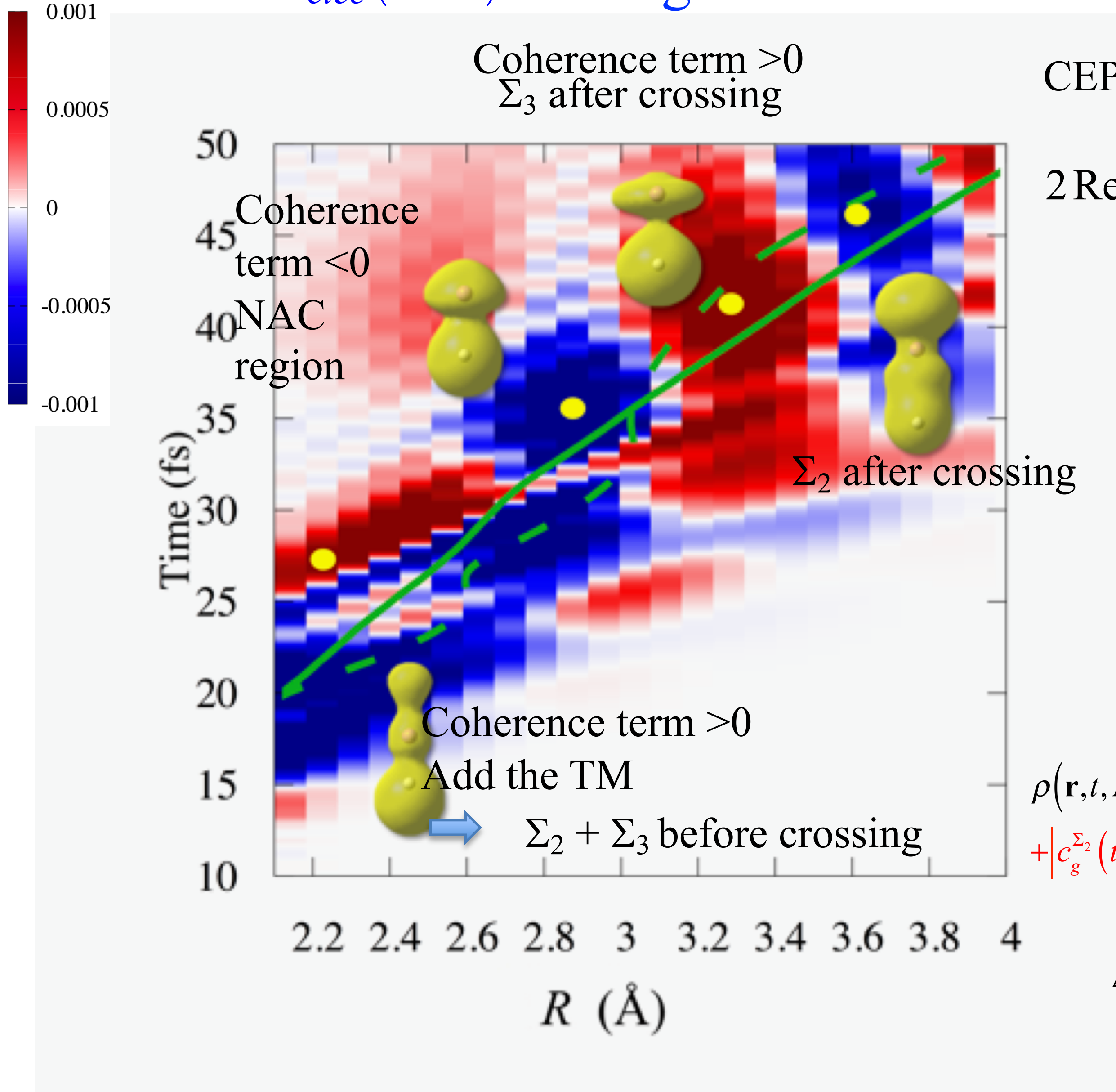

CEP=π $\mathrm{pop}\Sigma_2 > \mathrm{pop}\Sigma_3$

$$2\,\mathrm{Re}\left[c^*_{\Sigma 2,g}(t)\,c_{\Sigma 3,g}(t)\right]$$

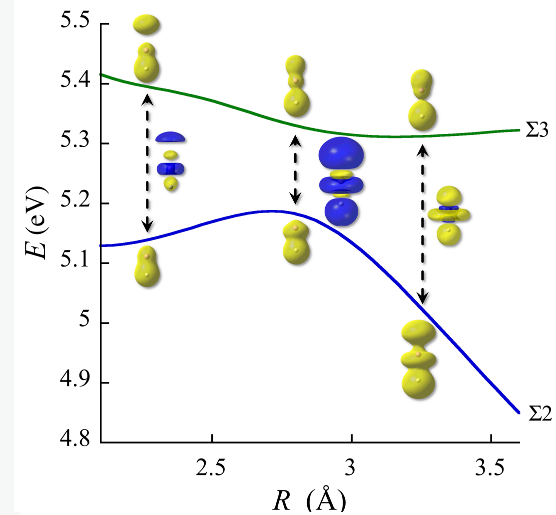

$$\rho(\mathbf{r},t,R_g) = \left|c_g^{\Sigma_2}(t)\right|^2 \rho_{\Sigma_2}(\mathbf{r};R_g) + \left|c_g^{\Sigma_3}(t)\right|^2 \rho_{\Sigma_3}(\mathbf{r};R_g)$$
$$+\left|c_g^{\Sigma_2}(t)\right|\left|c_g^{\Sigma_3}(t)\right|\cos\left(\Delta\phi_g(t)\right)\rho_{\Sigma_2-\Sigma_3}(\mathbf{r};R_g)$$

$$\Delta\phi_g(t) = \phi^g_{\Sigma_2}(t) - \phi^g_{\Sigma_3}(t)$$

Probing the Σ_2–Σ_3 coherence though the NAC region using MFPAD

Work in progress

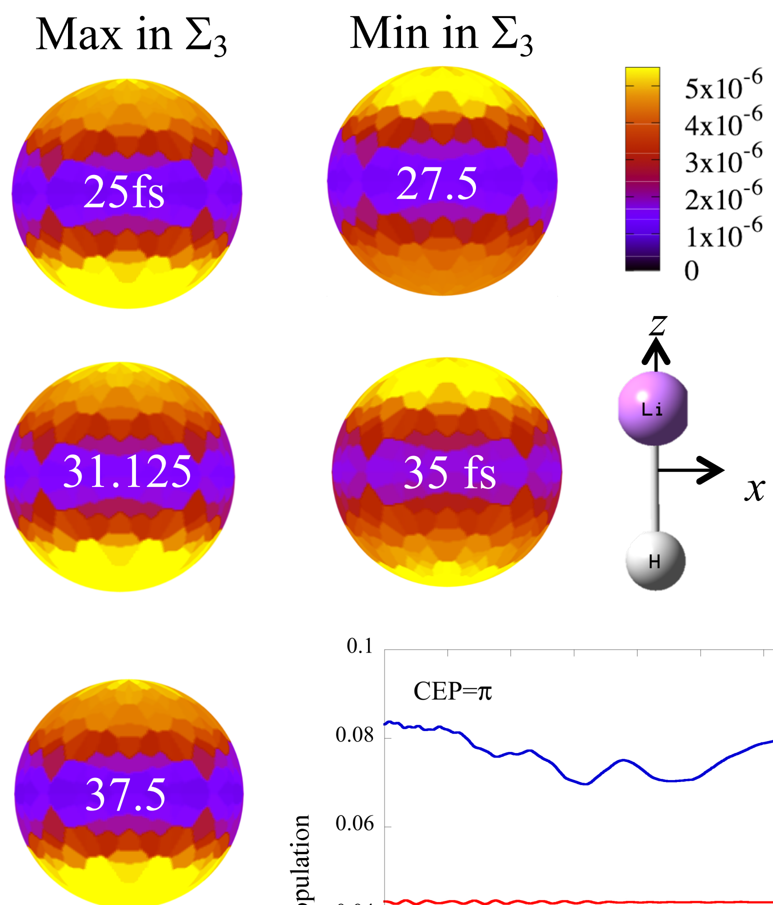

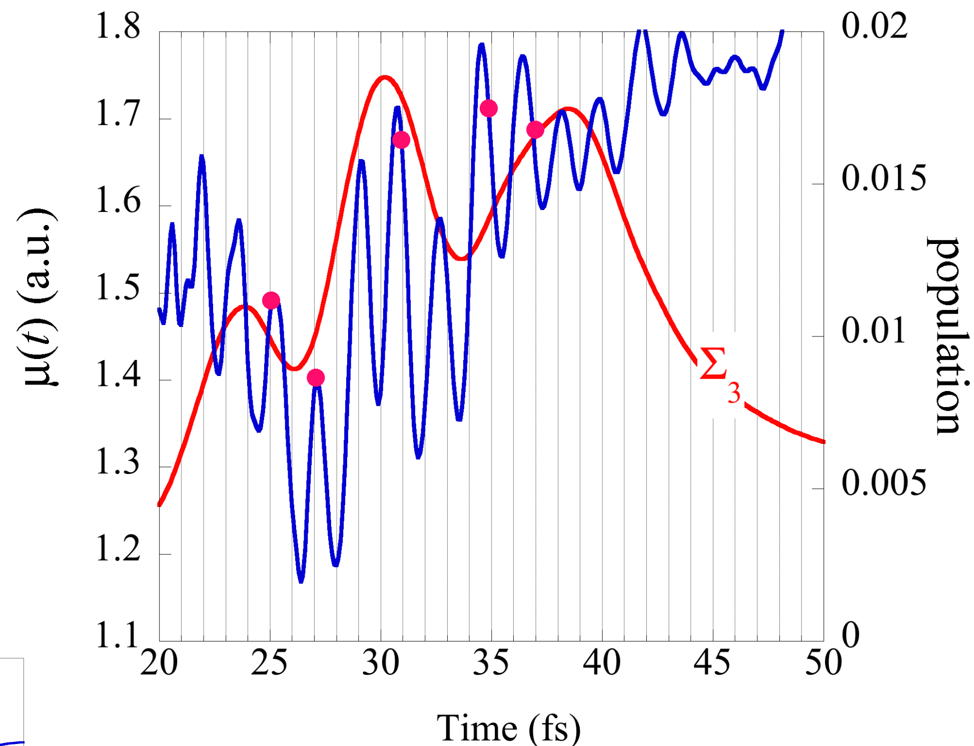

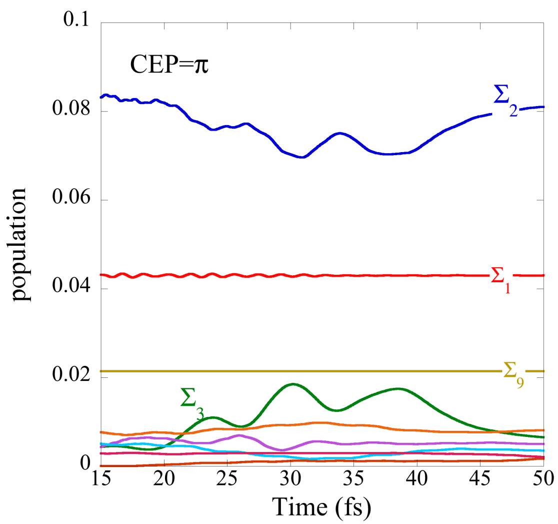

MFPAD averaged over nuclear coordinate for a kinetic energy of 12.65 eV

Probe : $|E_0|$=0.0075 au (1.9 10^{12} W/cm^2), σ=0.3 fs (FWHM = 0.7 fs), ω=0.72 au (19.6 eV)

Electronic coherence in HCN

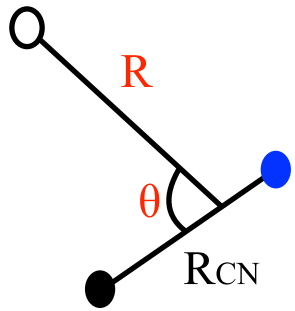

2D quantum dynamics in the internal coordinates R and θ on the GS and the first excited state

$$\hat{H} = -\frac{\hbar^2}{2\mu_H}\frac{\partial^2}{\partial R^2} - \frac{1}{2}\left(\frac{1}{\mu_H R^2} + \frac{1}{\mu_{CN} R_{CN}^2}\right)\frac{\partial^2}{\partial \theta^2} - \vec{E}(t)\cdot\hat{\mu}(R,\theta) + E_n^{el}(R,\theta)$$

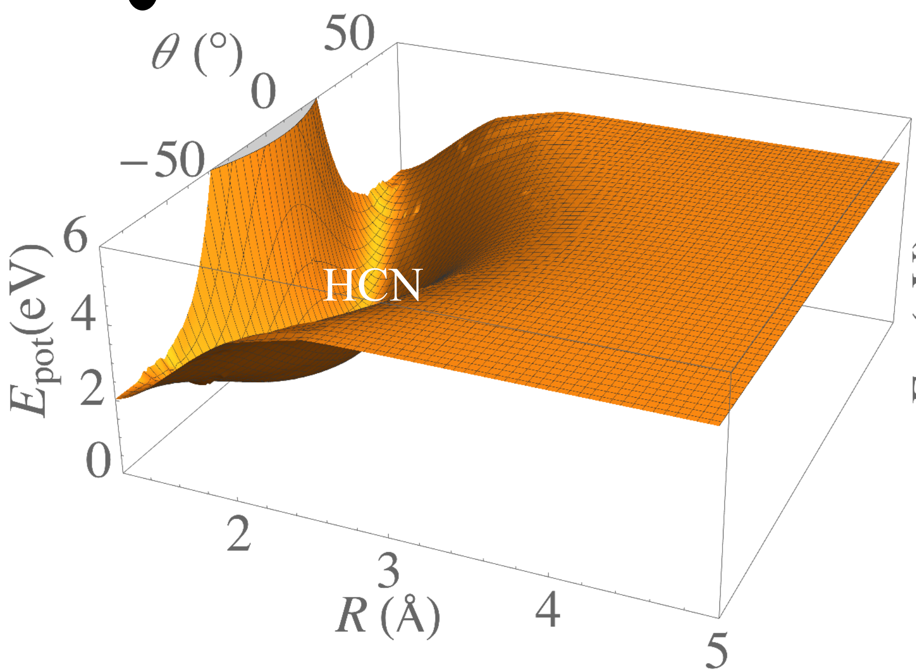

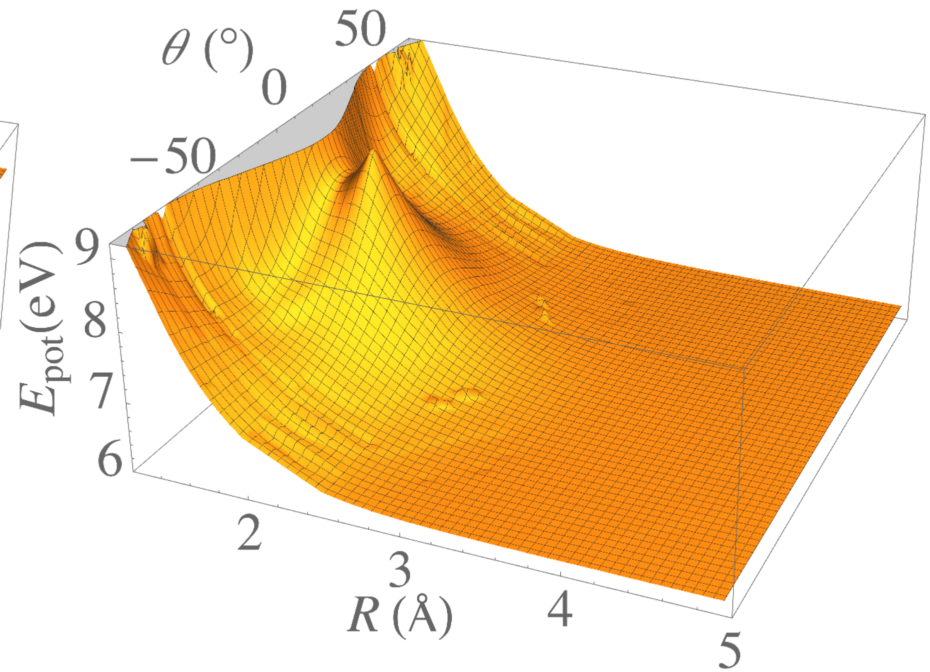

D^{calc}_0=42937cm^{-1}

D^{exp}_0=43740cm^{-1}

SA-CASSCF

CAS (10,12)

8 Excited states

Basis set: cc-PVTZ

Stephan van den Wildenberg, 2017

Dynamics

Excited states between 8.5 and 10 eV

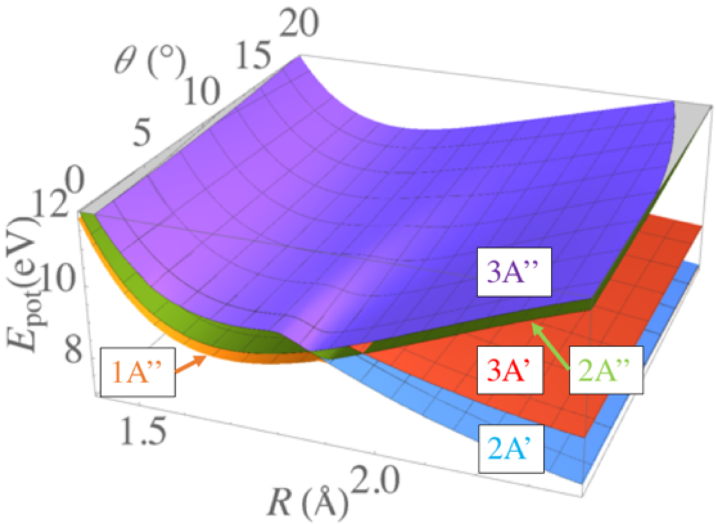

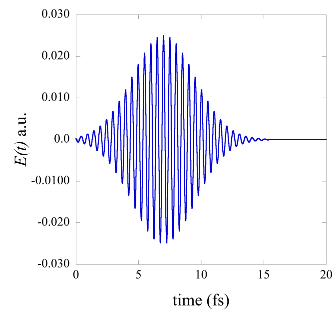

λ= 151 nm (8.16 eV)
0.5 eV below the first excited state
|E| = 0.025 au, σ=2.5 fs

Polarized perpendicularly to the molecular plane

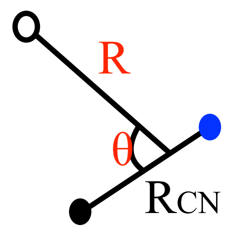

Transient dynamics

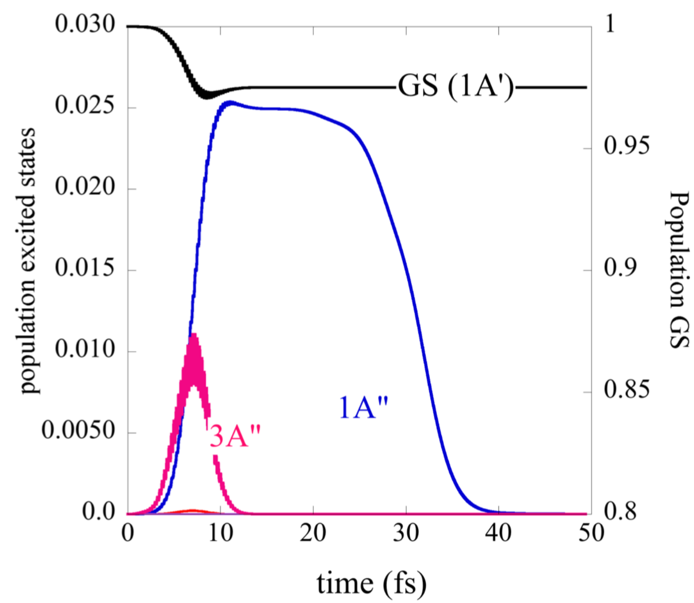

For θ ≠0, A' and A'' are coupled by the dipole interaction

During the pulse, we need to run the dynamics on 6 excited states

S. van den Wildenberg, B. Mignolet, R. D. Levine, FR PCCP, 9, 19837-19846 (2017).

Coherent motion in 2D on two electronic states

t = 20 fs

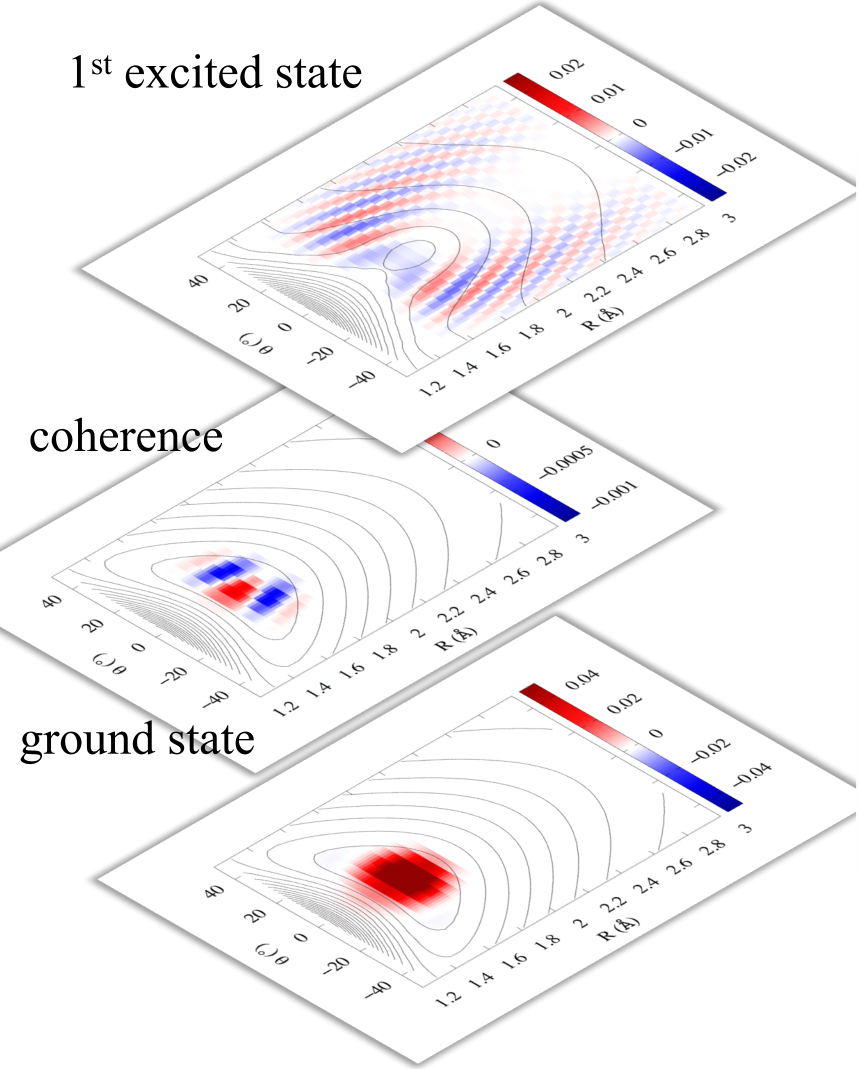

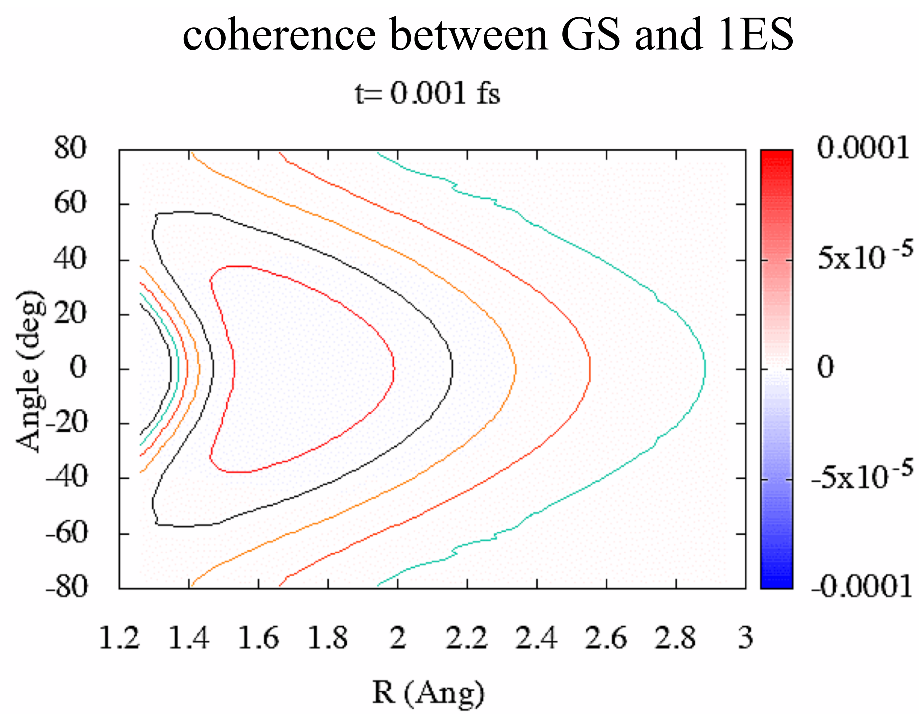

Observation of coherence between the GS and 1A”

Transient absorption spectra

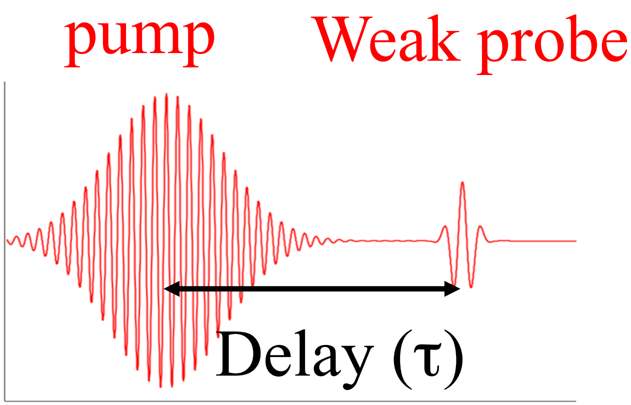

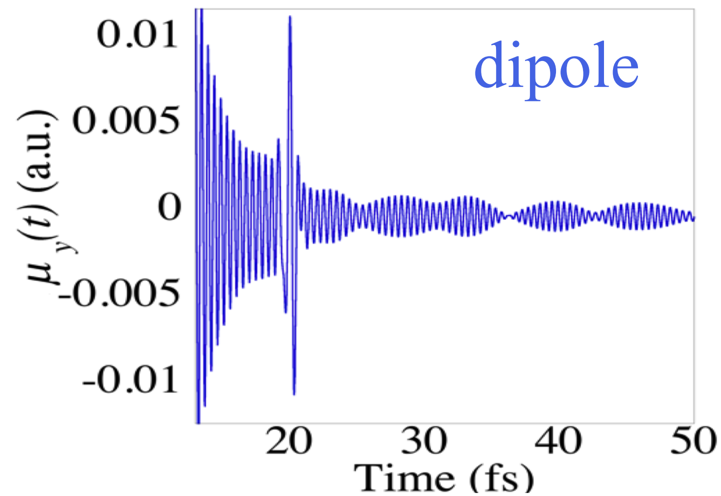

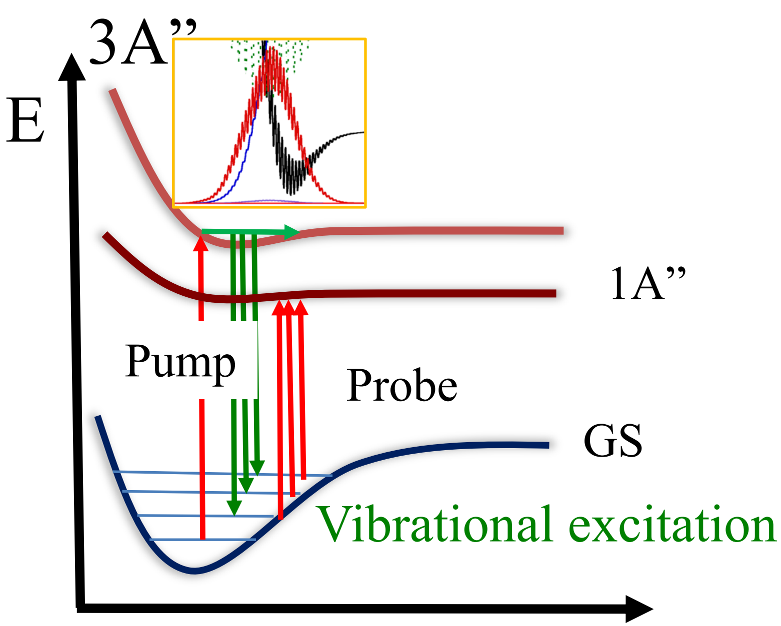

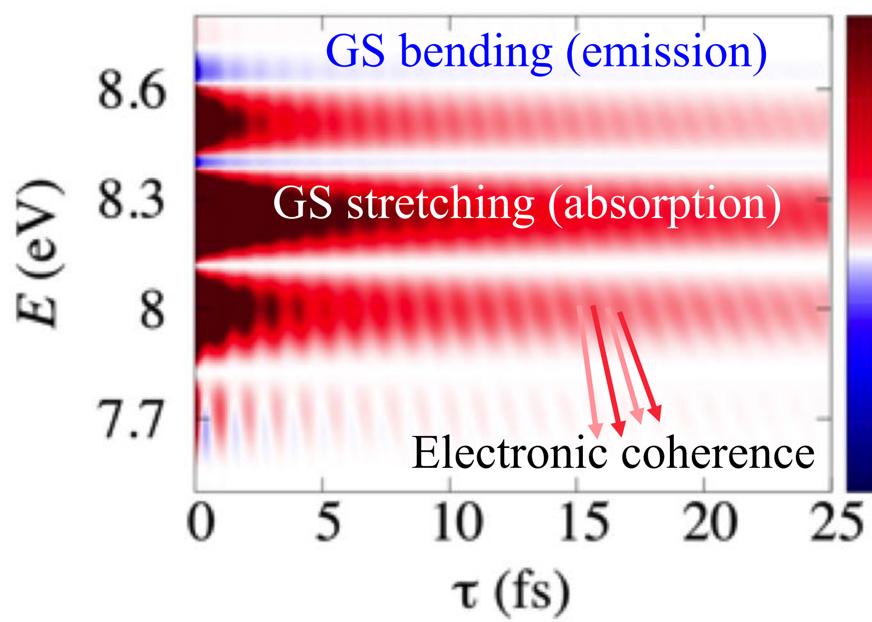

Quantum dynamics of the fast photoisomerization of norbornadiene

C_7H_8

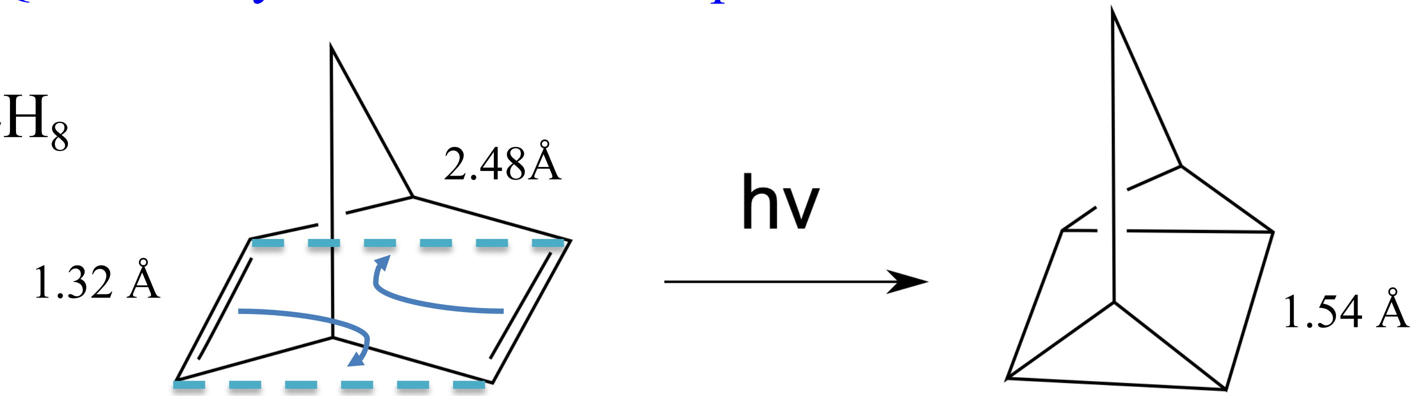

norbornadiene quadricyclane

Reduced dimensionality in three generalized coordinates (θ, γ, φ)

HC-CH_2-CH bridge is frozen

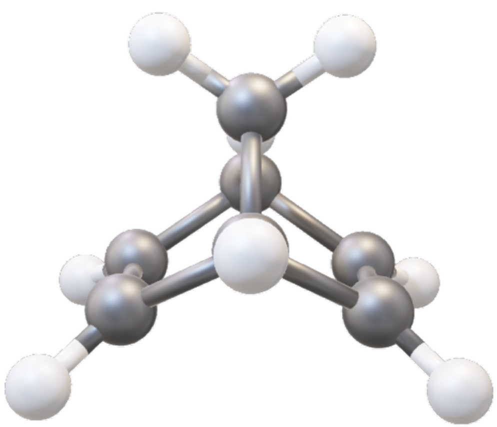

laboratory frame

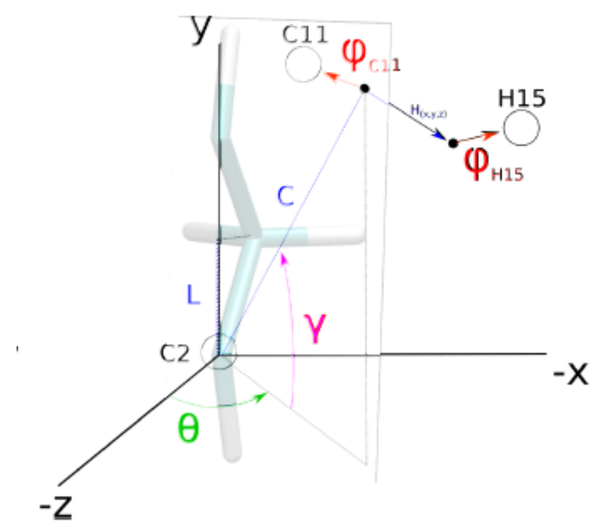

Dr. Alessio Valentini, ULiège, to be published

3D potentials

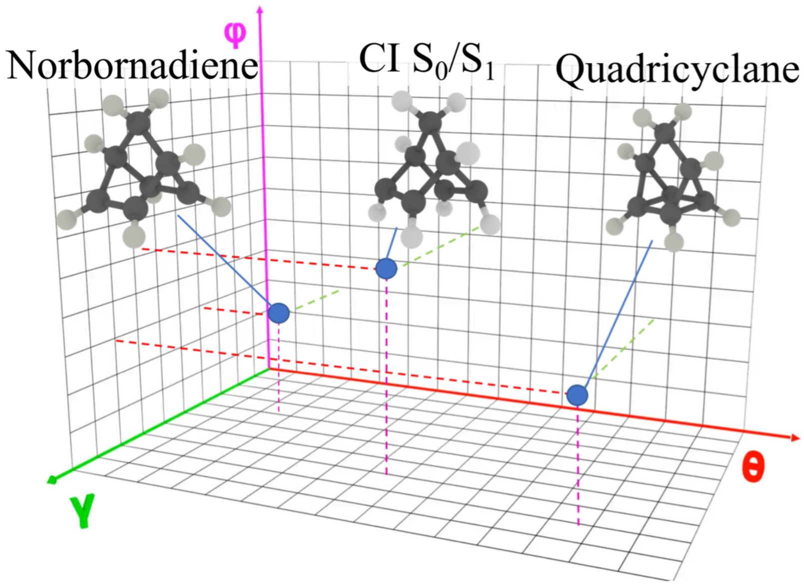

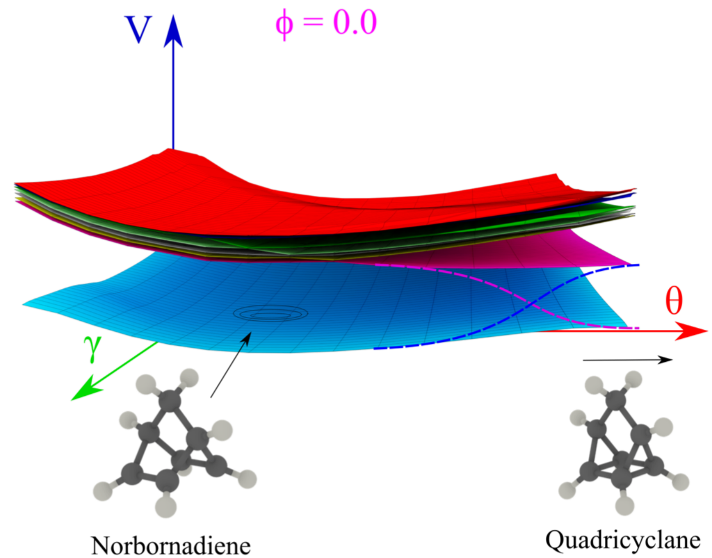

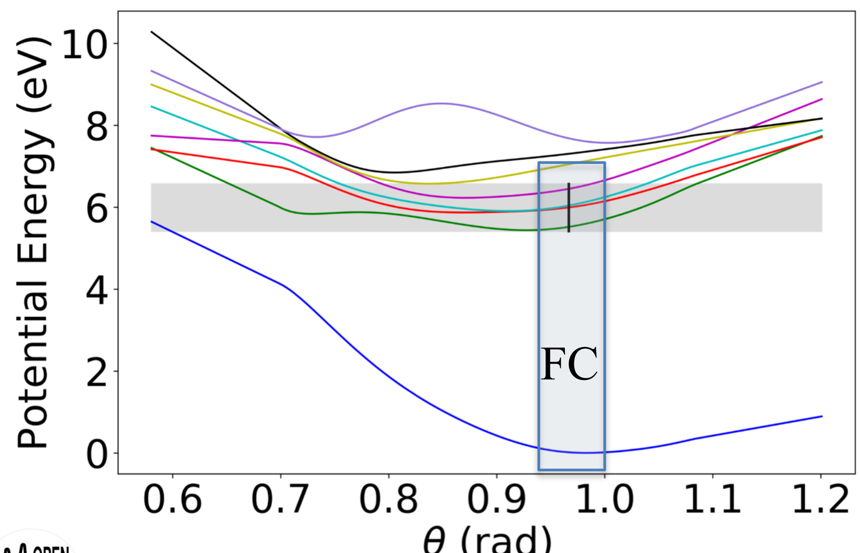

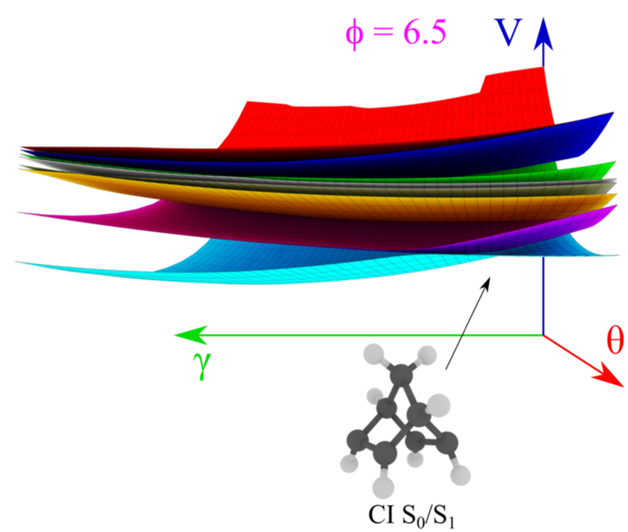

SA(14)-CAS(4,8)//AUG-CC-PVDZ

Electronic coherence at the vicinity of the CI

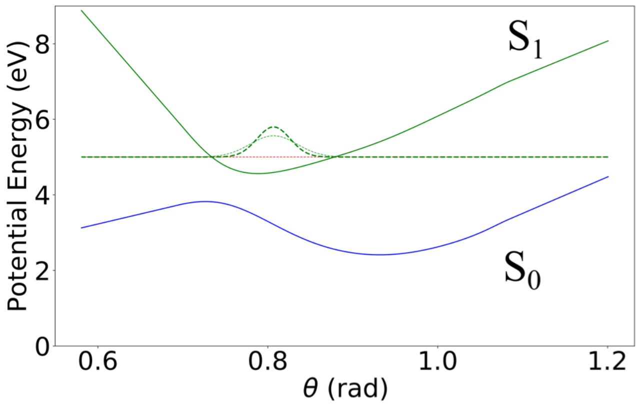

Nuclear wavepacket on S0 and S1

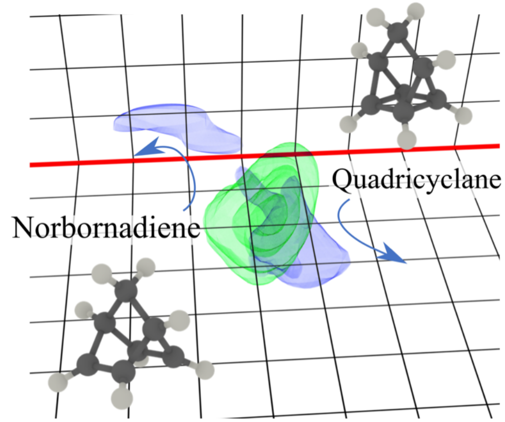

Vibronic S_0/S_1 Coherence

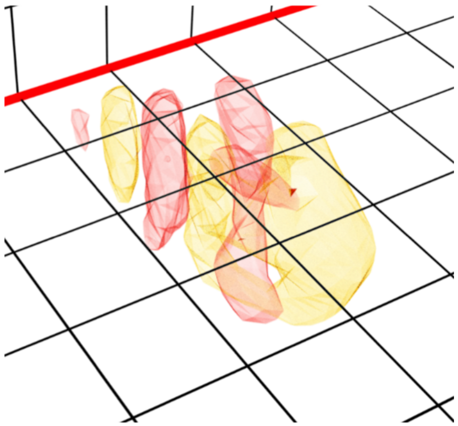

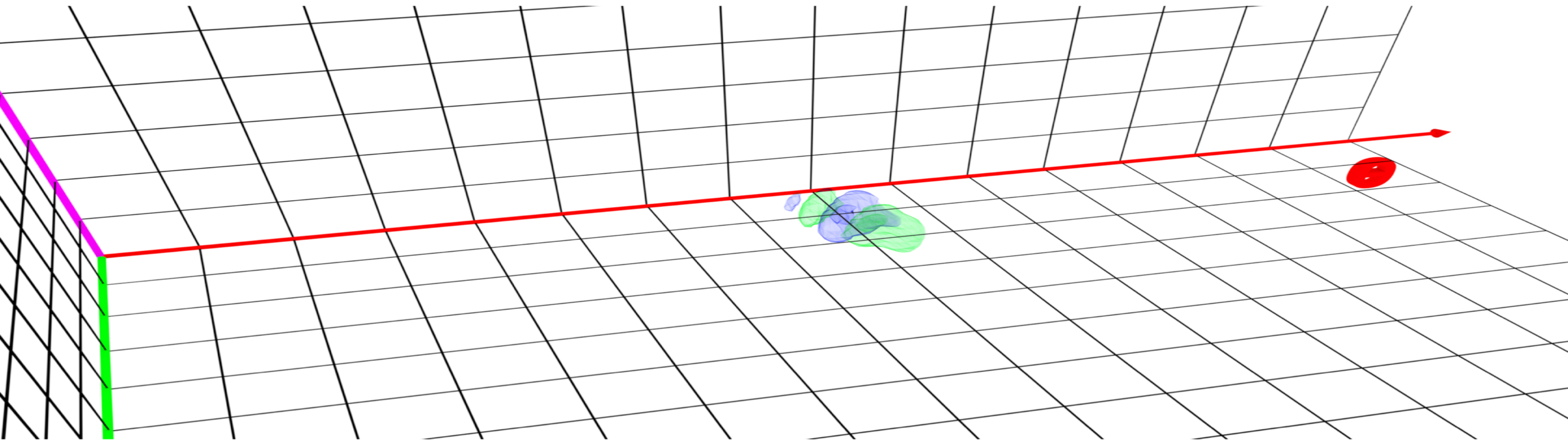

Conclusions and perspectives

- An electronic time scale before the onset of nuclear motion can be controlled and probed using attopulses.
- Dynamical simulations of the electron-nuclei dynamics in LiH show that one can implement a control of product yields tuning the pulse parameters (CEP, duration, field strength) in the presence of photoionization during the pulse and strong NAC coupling after the pulse.
- Dynamical simulations of electron-nuclei dynamics in Rydberg and valence states of N_2 show that electronic coherences govern a significant isotope effect.
- Electronic coherences created by the pulse are 'long lived'. They are modulated by nuclear motion and the NAC (in LiH, N_2, HCN and in norbornadiene).

Future work :

Implement the pump-probe scheme for 2 nuclear coordinates (HCN).

Investigate systematically the photoisomerization of norbornadiene.

Include Coulomb interactions in the photoionization description.

Funding :

fnrs
LA LIBERTÉ DE CHERCHER

U.S. DEPARTMENT OF ENERGY
Office of Science

Thank you

Thanks to my co-workers

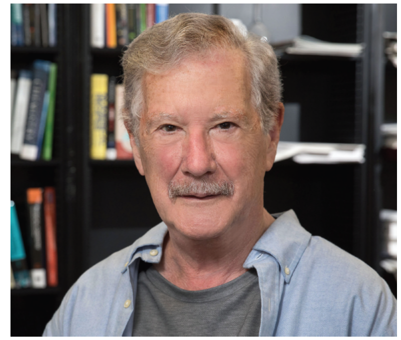

Raphael D. Levine

Dr. Ksenia Komarova

Dr Benoît Mignolet

Dr. Alessio Valentini

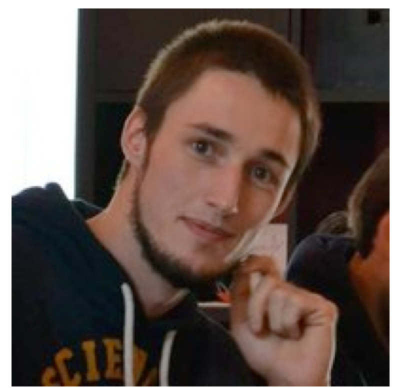

Stephan van den Wildenberg

Funding

U.S. DEPARTMENT OF ENERGY
Office of Science

fnrs
LA LIBERTÉ DE CHERCHER